



Studies on Hybrid Bio-Nanocomposites for Structural Applications

Vijayakumar Nimbagal, N.R. Banapurmath, Ashok M. Sajjan, Arun Y. Patil, and Sharanabasava V. Ganachari

Submitted: 31 December 2020 / Revised: 29 March 2021 / Accepted: 10 April 2021 / Published online: 18 May 2021

The present work emphasizes the synthesis of bio-nanocomposites using PLA and epoxy resin-based matrices through solution casting technique. An optimized 20% PLA-epoxy combination is further reinforced with nanofillers of graphene and multiwalled carbon nanotubes (MWCNTs). Dosage of the nanofillers is varied from 0.2 to 0.4 wt.% to develop bio-nanocomposites. Microstructure, characteristic studies such as SEM, TGA, and FTIR of the developed hybrid bio-nanocomposites are studied for the behavior of the novel material synthesized. From the experimental results obtained, hybrid bio-nanocomposites with 0.2 wt.% of graphene showed an increase in tensile and flexural strength, whereas MWCNT 0.3 wt.% showed an increase in tensile strength and 0.2 wt.% showed an increase in flexural strength compared to other weight percentages of both nanofillers (NFs). Further the SEM micrographs showed uniform distribution of NFs in the epoxy-PLA matrix. However, beyond 0.2wt.% of NFs dosage in the matrix the mechanical properties deteriorated due to non-uniform distribution of the nanofillers as seen in SEM micrographs. Experiments results are validated using FEM analysis for both hybrid bio-nanocomposites and epoxy/PLA composites. The results showed good agreement with an error of 10%. Hence 0.2 wt.% graphene and 0.3 wt.% MWCNT reinforced hybrid bio-nanocomposites could be used as an alternative material for automotive component applications.

Keywords Bio-nanocomposites, Epoxy resin, Finite Element Method (FEM), Graphene, Multiwalled Carbon Nanotubes (MWCNTs), PLA 3D printing Material, Polylactic acid (PLA), Scanning Electron Microscopy (SEM)

1. Introduction

Synthetic and biopolymer-based materials play prominent role in daily usage due to their extensive range of desirable properties. These polymers have high strength-to-weight ratio when compared to conventional materials (Ref 1). Due to the growing shortage of petroleum resources and their excessive pollution-related issues, the petroleum-based polymers need to

be suitably replaced with environmental friendly and biodegradable materials (Ref 2–4). Use of nanotechnology and nanomaterials are gaining prominence due to their exceptionally desirable properties when compared to their relative micro-based materials. Nanocomposites are widely researched materials, and the dispersion of fillers in the holding matrix is still a challenging process for infusion of higher dosage of NPs as it leads to aggregation. Researchers are exploring feasible solutions to ensure uniform distribution of nanofillers in the holding matrix with different techniques. Polymer nanocomposites is showing tremendous potential as a future material in various engineering applications due to their superior consistency, structural, electrical, and mechanical properties (Ref 5–7).

Epoxy is a thermosetting polymer and can be considered as a matrix, adhesive, and coatings to obtain versatile properties such as mechanical, thermal, and low density and suffers from high brittleness. Reducing the brittleness of the epoxy-based material is carried out by several researchers to enhance its ductility. Epoxy-based nanocomposites find wide applications in automobiles, aircraft, athletic equipment, marine, biomedical devices.

Development of lightweight nanocomposites using graphene (Gr) and multiwalled carbon nanotubes (MWCNTs) find different applications with higher mechanical, electrical, thermal and optical properties. Higher dosage of graphene nanoplatelets (GNP) and amine-functionalized graphene nanocomposites showed improved mechanical properties when compared to unfunctionalized graphene material. Enhanced tensile strength was demonstrated by amine-functionalized nanocomposites which were more brittle than neat epoxy. This is due to aggregation of nanoplatelet graphene (Ref 8).

Epoxy composites with functionalized carbon nanotubes (CNTs) and GNPs composite were analyzed for specific applications and accordingly 2 wt.% GNP nanocomposites

This invited article is part of a special topical focus in the *Journal of Materials Engineering and Performance* on Additive Manufacturing. The issue was organized by Dr. William Frazier, Pilgrim Consulting, LLC; Mr. Rick Russell, NASA; Dr. Yan Lu, NIST; Dr. Brandon D. Ribic, America Makes; and Caroline Vail, NSWC Carderock.

Vijayakumar Nimbagal, School of Mechanical Engineering, B.V.B. College of Engineering and Technology, K.L.E. Technological University, Vidyanagar, Hubballi 580031, India; **N.R. Banapurmath** and **Arun Y. Patil**, Centre for Material Science, B.V.B. College of Engineering and Technology, K.L.E. Technological University, Vidyanagar, Hubballi 580031, India; and School of Mechanical Engineering, B.V.B. College of Engineering and Technology, K.L.E. Technological University, Vidyanagar, Hubballi 580031, India; and **Ashok M. Sajjan** and **Sharanabasava V. Ganachari**, Centre for Material Science, B.V.B. College of Engineering and Technology, K.L.E. Technological University, Vidyanagar, Hubballi 580031, India. Contact e-mails: nrbanapurmath@gmail.com and sharanu14@gmail.com.

showed improved properties compared to one-dimensional CNTs. The reinforcement effects of the two-dimensional GNPs were stronger than those of one-dimensional GNPs because of differences in pull-out processes and bridging effects of CNTs. (Ref 9) Size, orientation, interaction, and dispersion of nanoparticles play a significant role in the development of nanocomposites. Graphene with good mechanical and thermal properties, find applications in mechanical and microelectronic devices (Ref 10).

Orientation of nanoparticles has a significant role in improving mechanical and thermal behavior of epoxy resin with magnetic composite consisting of GO, MWCNTs and Fe₃O₄. Orientation was controlled by magnetic field, and the results showed improvement of mechanical properties for 1.5% wt. of GMF bending strength has improved by 136.5% and impact strength by 30.9%. (Ref 11)

Several researchers focused on the effect of reinforcing two nanofillers (hybrid nanocomposites) with varying dosages in synthesis of polymer nanocomposites. Epoxy-based hybrid composites were reinforced with O₂-functionalized GNP and MWCNT as nanofillers. Dosage of GNP was varied from 2, 4, 8 and 10, with 0.5%, while MWCNTs is kept constant in an epoxy matrix. Hybrid composites with 10% GNP showed improvement in compressive strength by 260% and 190% increase in tensile strength. Microstructure structure analysis carried out showed even distribution of GNP and MWCNTs in the matrix of epoxy (Ref 12). Hybridization of glass and Kevlar fiber on thermal properties of epoxy matrix was studied using TGA and DSC test and found improved the transition temperature and thermal properties (Ref 1,13-15). Comparative study of epoxy nanohybrid coatings using aminosilane-functionalized ZnO with varied dosages of 1,3,5 and 7% in a matrix of diglycidyl ethers bisphenol was studied. 3% ZnO was found to be optimum dosage with improved thermal properties when compared with epoxy-based nanocomposites (Ref 16).

Natural fibers as fillers in the epoxy matrix have gained attention by several researchers due to their environment friendly, low cost, and reduced health hazards when compared to synthetic carbon and glass. Natural fiber composites showed improved mechanical properties such as tensile strength, flexural, and toughness (Ref 17). Effect of reinforcing natural fibers like palm, birch, and eucalyptus in an epoxy matrix with a dosage of 35 wt.% has been reported in the literature. Compared to other fibers such as palm and birch, the combination of resin transfer molding and molded fiber-based processing technique provided greater tensile strength with eucalyptus/epoxy among the three varieties (Ref 18). Use of natural and synthetic fillers at both nano- and microlevel in the epoxy-based composites has been investigated for structural application. Hybrid epoxy matrix-based composites reinforced with synthetic filler graphene by 0.3 wt.% and hemp treated with NaOH and KMnO₄ using dosage 5 wt.% showed higher strength compared to neat epoxy (Ref 19–22). Further effect of sweet lime and lemon particles in an epoxy matrix using varied dosages has been investigated, and epoxy with lemon particle of 30% volume fraction showed enhanced mechanical properties compared to pristine epoxy (Ref 23). The dynamic and structural properties of the jute/epoxy-based matrix with ZnO and TiO₂ nanofillers were investigated. Properties of epoxy and jute with 4 wt.% of TiO₂ composites were tested at both room and subzero temperature, and the combination showed enhanced tensile and compressive strength (Ref 24).

Epoxy-based matrix composites reinforced with silica nanoparticles (SNs) and epoxidized natural rubber (ENR) as fillers were used for blades of drones due to their resistance to weather and enhanced mechanical properties (Ref 25). ENR showed a reduction in glass transition temperature (T_g) and epoxy resin modulus, with a slight improvement in modulus when combined with SN. Silica nanoparticles addition assisted in toughening of the epoxy matrix. Yield strength decreased as ENR percentage increased. Yield strength increased as the SN's percentage increased when epoxy was mixed with hybrid SN. ENR does not improve interfacial strength between matrix and epoxy compared to neat epoxy (Ref 26). Epoxy-based hybrid composites exhibited good fire-resistance and enhanced structural properties and find applications in the aerospace industry, and fire-resistance casing for electrical devices (Ref 27). Thermomechanical properties of nanocomposites were studied reinforcing h-BN in the epoxy, and 5 wt.% epoxy showed higher glass transition temperature with improved Tensile, impact, storage modulus properties, while increase in h-BN content showed higher surface roughness (Ref 28). Several researchers studied the thermal stability of hybrid composites using addition of silicon carbide (SiC) nanoparticle in an epoxy/graphene amine (GA) matrix. Tensile strength showed maximum elongation for 0.75% of SiC in an epoxy/GA, and it reduced with an increase in SiC wt.% because of higher brittle nature of SiC (Ref 29).

Hybrid composites were prepared using jute fibers and cenosphere as fillers with their varied dosage. Tensile properties of jute with 4 layers showed significant improvement with addition of cenosphere. Increase in the percentage of jute and cenosphere percentage resulted in the decreased thermal conductivity of the composites developed. (Ref 30)

Epoxy as the most appropriate thermoset resin is commonly used for reinforcement of organic, inorganic and natural fibers as fillers at micro- and nanostages, ranging from household to engineering applications (Ref 5,31-33). Table 1 illustrates the mechanical properties of composites based on epoxy.

The use of synthetic polymer products has increased significantly, leading to environmental pollution and health hazards for human beings as they are non-degradable. A suitable biodegradable material that can replace non-degradable polymer composite is the need of the hour. In this direction PLA finds tremendous potential as an alternative to petroleum based products (Ref 34). A synergistic combination of biopolymer and synthetic polymer facilitated by robust interfacial interactions and controlled dispersion can reduce environmental pollution. Bio-composite has diversified applications in the areas of medical, textile, electronics, packaging, and food processing industries. Poly lactic acid (PLA) has become an extensively used biopolymer material derived from renewable sources like corn starch and sugarcane. PLA has diverse applications ranging from plastic films, bottles, and medical devices PLA is the most widely used plastic filament material in 3D printing. PLA has weak mechanical and thermal properties and requires reinforcement of inorganic/organic/natural fibers to improve its mechanical, thermal properties. Interrelation between microstructure and macroscopic behavior of composites is the basis for a specific application and properties (Ref 35).

PLA is blended with polycarbonate (PC), nanosilica and catalysts such as cobalt (Co) and dicumyl peroxide (DCP) to reduce its brittleness. PLA/PC/Silica composites showed improved thermal stability, higher percentage of elongation

Table 1 Optimum dosage, mechanical properties of epoxy-based composite/hybrid composite

| Composite | Process of manufacturing | The optimum dosage of nanofillers | Investigated properties: percentage of improvement of property compared to neat epoxy | References |
|---|---|---|--|--|
| GO/CNT/WEP Epoxy (0.5wt.%) + (75Gr:25ND) Epoxy (0.8 wt.%) + Toughness:140 Tensile: 51 Fracture Toughness:165 | The aqueous solution mixing method (25Gr:25CNT:50ND) (Ref 66) | 1% of GO/CNT/WEP Solution casting method | Tensile: 28 0.8 wt.% | (Ref 65) Tensile: 46 Fracture |
| Epoxy+Gr+MWCNT | Direct mixing method | 0.5 wt.% (9:1) | 59 (with GNP) 27(with MWCNT) | (Ref 67) |
| Epoxy+GO+ CF | Solution casting | 0.3 wt.% | Tensile strength: -25 Bending strength: -66 Shear strength:25 | (Ref 68) |
| Epoxy +Al ₂ O ₃ | Solution blending | 1 wt.% | Flexural strength: -15 | (Ref 69) |
| Epoxy +Kevlar +Pulp | Solution casting | Kevelar -0.3% | Tensile strength:117 | (Ref 70) |
| Epoxy/onion peel Epoxy/potato Epoxy/carrot | Hand lay-up | 10% | Flexural strength :113 Flexural -36.06MPa Hardness -50.75 HRB Flexural -35.00MPa Hardness -49.75 HRB Flexural -34.55 MPa Hardness -37.75 HRB | (Ref 61) |
| Epoxy+TCSE | Hand lay-up and compression molding | 5 Layers of coconut sheath | Tensile strength:21.19 Flexural: 18.88 Impact test:24.39 | (Ref 71) |
| Epoxy+h-BN | Stir casting | 0.5 wt.% | Tensile strength:-35 Impact strength:-60 | (Ref 28) |

Graphene oxide (GO), carbon nanotube (CNT), waterborne epoxy (WEP), graphene (Gr), carbon nanotube (CNT), nanodiamond (ND), multiwalled carbon nanotube (MWCNT), carbon fiber (CF), treated coconut sheath epoxy (TCSE)

and reduced tensile strength compared to pristine samples of PLA and PLA/PC. Higher percentage of elongation was achieved due to catalytic efficiency of both Co and DCP. (Ref 36).

Influence of reinforcement in different dosages on the PLA composites with reference to mechanical and thermal degradation properties was studied. PLA was modified with poly (butylene adipate-co-terephthalate) (PBAT), which functions as a CNT-COOH nanoparticles-reinforced matrix. Increased tensile strength was obtained for 0.5wt% of CNT-COOH nanoparticles dosage in the matrix, while decreased trends were obtained beyond 0.5wt percent infusion due to self-aggregation of CNT-COOH nanoparticles. TGA test on the composites showed increased decomposition temperature with higher percentage of CNT-COOH and is due to the addition of nanoparticles that prevented the transport of elements in the composite material. (Ref 34).

In another work mechanical, thermal properties of Gr reinforced with PLA was studied to analyze the effect of exfoliated expandable graphene (EG) at around 750°C. The TGA test showed 10 percent weight loss and the thermal stability of PLA-Gr increased by 60°C, while the tensile strength of PLA-Gr demonstrated improvement relative to pristine PLA-Gr. (Ref 37).

Apart from structural applications, PLA is also being used as bioresorbable implant material for orthopedic inner fixation (Ref 38). In another applications on construction, PLA is used

as a replacement material for fine cement mortar aggregates. Mechanical and biodegradation studies were carried out by replacing fine aggregates with PLA in various percentages ranging from 0 to 50% and the resulting specimens were tested for mechanical and biodegradation tests. Tensile and compressive strength were improved for 10% PLA replacement. Simultaneously, the biodegradability test of PLA granules showed that the failure pattern for the specimen buried for 7 days showed no degradation to PLA granules. PLA granules reinforced specimens of 28 days showed that PLA granules are undergoing degradation. In another work, degradation study on PLA was done by coating with epoxy for better durability. The results were encouraging for 0.1-0.4 percent difference relative to the actual weight of the specimens considered (Ref 39).

PLA being biodegradable, and lightweight can be reinforced with natural fibers to develop low-cost material. Biopolymers reinforced with natural fibers of Jute, hemp, kenaf, ramie, cotton, coir, palm were studied in depth to ascertain their feasibility as an alternative material for structural applications. Use of untreated natural fibers in the PLA matrix composites showed decreased impact strength due to poor interfacial adhesion between the fiber and the matrix. On the other hand, treated surface of natural fibers in PLA and flexible epoxy showed an increase in impact properties relative to untreated composites (Ref 40). PLA reinforced with natural fibers such as Kneaf (PLA/kenaf) and Rice Husk (PLA-RH) showed decreased flexural and impact strength due to irregular form

and week interfacial bonding between matrix and fiber. Compared to pristine PLA, increased flexural modulus of the composites with natural fiber were found due to stiffer reinforcing material used in the matrix. PLA/Kneaf biodegradability was found to be significantly higher than that of PLA-RH. (Ref 41).

Thermomechanical properties of PLA composites were studied by varying dosages of fibers from 10 to 40 percent, and the resulting composite was studied for tensile and interfacial adhesion. Composites reinforced with fiber by 20 wt.% showed promising results. Further the Einstein and van dyack model used provided good agreement in the results in terms of mechanical behavior (Ref 42).

Studies reported that composites of natural fibers/PLA treated with epoxy showed an improvement in impact strength compared to untreated natural fiber /PLA composites. Another work reported on the biodegradability of epoxy coated PLA, which had shown improvement in the biodegradability/durability of PLA, replacing aggregates in concrete. It was observed from the previous works which are reported that PLA surface treated with epoxy has improved impact strength and biodegradability of PLA.

From the exhaustive literature survey carried out, it is found that the hybrid nanocomposites using combination of PLA and epoxy as matrix has not been reported. Hence, the objective of the present work is to mainly synthesize nanocomposites using 20% PLA for partial replacement of the epoxy resin. Further the research work on hybrid bio-nanocomposites reinforced with nanofillers has been scantily reported in the literature.

In view of this, an attempt has been made to optimize the percentage of PLA in epoxy and accordingly 20 wt.% of PLA in epoxy was optimized in terms of better mechanical strength as reported by authors earlier work (Ref 43). 20 wt.% of epoxy-PLA biopolymer-based composites are reinforced with nanofillers such as Gr and MWCNT in varying dosage. The dosage of NFs is varied from 0.2 to 0.4 wt.%. Further, these epoxy/PLA-based bio-nanocomposites are evaluated for mechanical, thermal, and morphological characteristics.

2. Experimental

The materials and procedures used to prepare composites and research methods adopted in the characterization of composites are discussed in this section.

Table 2 Epoxy resin L-12 material properties

| Material | Value | Unit |
|----------------------|-------------------------------|-------------------|
| Commercial name | Lapox, L-12 | ... |
| Density | 1162 | Kg/m ³ |
| Tensile strength | 50-60 | MPa |
| Compressive strength | 110-120 | MPa |
| Flexural | 130-150 | MPa |
| Minimum curing time | 14-24 hrs at temperature 25°C | ... |
| Viscosity | 9000-12000 at 25°C | m Pa.s |

2.1 Materials

Epoxy resin L-12 was chosen from Atul India Ltd Ahmedabad, Gujarat, India, is used, and its properties are shown in Table 2. PLA 3052 D is sourced from Nature Works, USA, and its physical and mechanical properties are shown in Tables 3 and 4, respectively. Graphene and MWCNT are chosen as fillers procured from United Nanotech Innovation Pvt Ltd Chokkahalli Village Karnataka. The properties of Graphene and MWCNT are depicted in Tables 5 and 6.

2.2 Methods

The process flow depicted in Fig. 1 shows the methodology followed in the present work. Solution casting techniques (SCT) are used to prepare the composites. SCT ensures the uniform distribution of nanoparticles in to the matrix and it is a low temperature process and it is a suitable process to prepare bio-based composites (Ref 44). SCT the polymer phase is dissolved in water or a non-aqueous volatile solvent and combined with nanosized reinforcements in the same solvent medium. The solvent is separated by evaporation, and the dried film is then removed from the substrate (Ref 45). Initially, a known quantity of epoxy was taken, which is heated to reduce its viscosity. PLA, which is in the granules form, is dissolved in

Table 3 Physical properties of PLA

| Physical characteristics | Value | Unit |
|--------------------------|-----------|-------------------|
| Melting temperature | 120-170 | °C |
| Load | 2.16 | Kg |
| Specific gravity | 1.25 | ... |
| Bulk density | 1250 | Kg/m ³ |
| Particle Size | 1.18-4.75 | Mm |
| Shape | Rounded | ... |
| Texture | Smooth | ... |

Table 4 Mechanical properties of PLA

| Properties | Value | Unit |
|---------------------------|-------|-------------------|
| Density | 1.25 | Kg/m ³ |
| Tensile strength at yield | 62 | MPa |
| Flexural modulus | 3600 | MPa |
| Flexural strength | 108 | MPa |
| Elastic modulus | 1287 | MPa |

Table 5 Properties of graphene

| Properties | Value | Unit |
|------------------|-------|---------|
| Bulk density | 0.24 | g/cc |
| Diameter average | 5-10 | Microns |
| Carbon purity | >99% | ... |
| Tensile strength | >5 | Gpa |
| Tensile modulus | >1000 | MPa |

THF solution, and then the K-6 hardener is added to the mixture to have good adhesion between PLA and epoxy. Epoxy and PLA combination is obtained by varying dosages of PLA from 10 to 30 wt.% in steps of 10. However, in the present work only 20 wt.% of PLA in epoxy-based composite is presented for the analysis.

2.3 Preparation of Hybrid Nanocomposites

Hybrid bio-nanocomposites are been processed by optimized percentage of PLA in epoxy (20 wt%) reinforced with nanoparticles such as Gr, and MWCNT is used to synthesize hybrid nanocomposites. The process flow in the synthesis of nanocomposite is depicted in Fig. 2.

Initially, the nanoparticles graphene and MWCNT with a dosage of 0.2,0.3 and 0.4%. wt. are dissolved separately in 10 ml ethanol solution for 10minutes in an ultra-sonicator and kept for 10 minutes to have a uniform distribution of nanoparticles. Then Gr and MWCNT nanoparticles are mixed with epoxy resin with constant stirring and are held in an ultra-sonicator for 50 minutes to evaporate the alcohol content in the mixture. Further, the mixture is added with PLA and K-6 Hardener, and finally, it is poured into the molds of size 230mm × 160mm ×

3mm and kept 24 hrs for curing of the specimens. The details of the different test specimen used in the study are shown in Table 7.

3. Characterizations

3.1 Materials Characterization

FTIR experiments are performed using agate mortar to prepare the powder sample of bio-composites. KBR pellets are made using the powder sampled from the PLA-epoxy make spectrum Perkin-Elmer. TGA experiments are carried out using SDT Q600 TA Instruments, USA, to determine thermal degradation, oxidative stability of the samples. Microstructural analysis of the bio-nanocomposites is carried out using Carl Zeiss EVO 18 Research SEM.

3.2 Mechanical Testing

3.2.1 Tensile Testing. The tensile test is carried out to determine the maximum load the specimen can withstand and also to know the maximum deflection the specimen undergoes at this load. From these data, the yield strength and modulus of elasticity are determined. The tensile test is carried out using a Micro Universal Testing Machine (UTM) Supplied by Enkay Enterprises, Bangalore, with a capacity of 10kN. The specimens were prepared according to ASTM D638. The size of the sample specimen is 165 mm × 19 mm × 3 mm. A uni-axial load is applied through both ends. The tensile specimen's gauge length is 138 mm, and a crosshead speed of 3 mm/min is fixed (Ref 46-50).

Table 6 Properties of MWCNT

| Properties | Value | Unit |
|------------------|-----------|-------------------|
| Bulk density | 0.04-0.06 | g/cm ³ |
| Diameter average | 5-20 | nm |
| Nanotubes purity | > 90 | ... |
| Amorphous carbon | < 1% | ... |

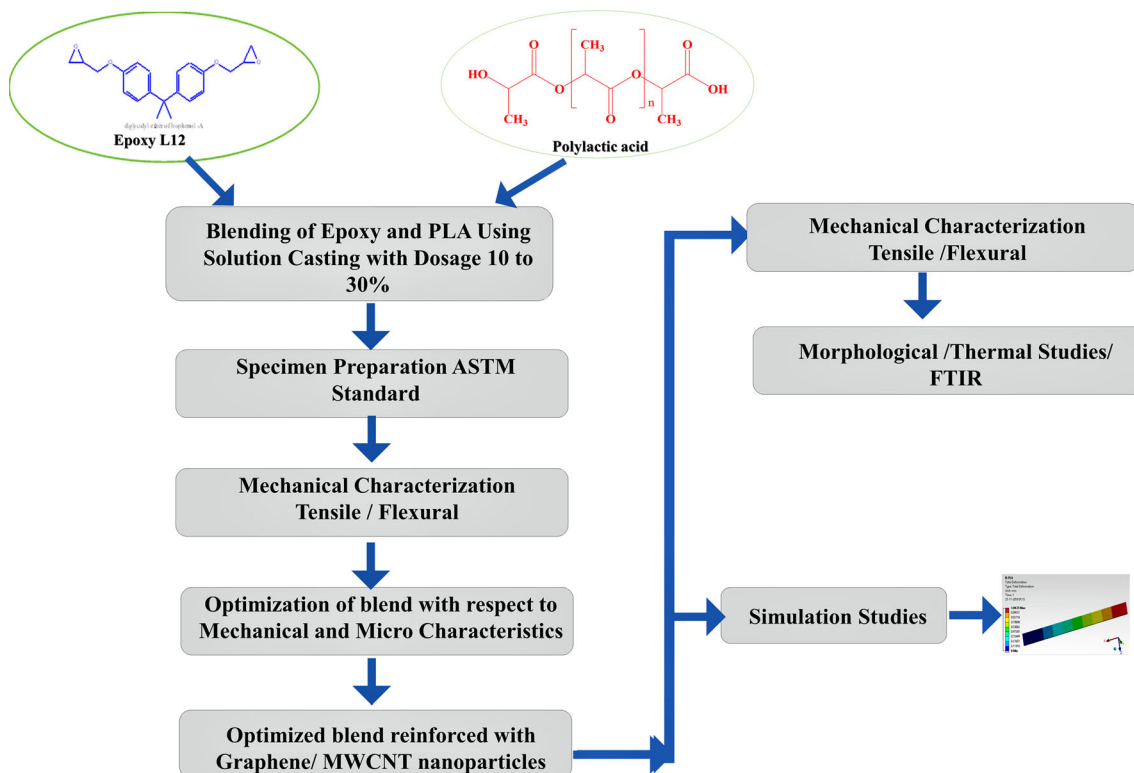


Fig. 1 Methodology of epoxy/PLA reinforced with nanoparticles

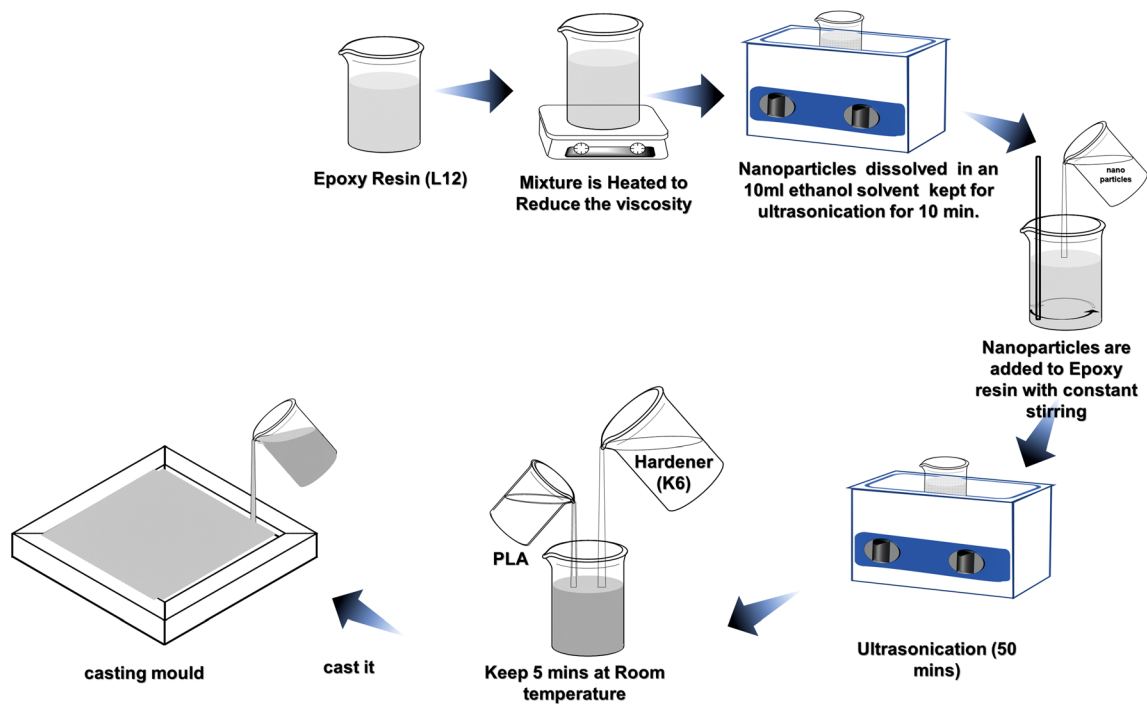


Fig. 2 Process flow nanocomposite preparation

Table 7 Details of test specimen

| S. no. | Sample codes | Epoxy, wt. % | PLA, wt. % | Graphene, wt. % | MWCNT, wt. % | Remarks |
|--------|--------------|--------------|------------|-----------------|--------------|------------------------|
| 1 | B10 | 90 | 10 | ... | ... | Previous reported work |
| 2 | B 20 | 80 | 20 | ... | ... | “ |
| 3 | B 30 | 70 | 30 | ... | ... | “ |
| 4 | BG 0.2 | 79.9 | 19.9 | 0.2 | ... | Present work |
| 5 | BG 0.3 | 79.85 | 19.85 | 0.3 | ... | “ |
| 6 | BG 0.4 | 79.8 | 19.8 | 0.4 | ... | “ |
| 7 | BM 0.2 | 79.9 | 19.9 | ... | 0.2 | “ |
| 8 | BM 0.3 | 79.85 | 19.85 | ... | 0.3 | “ |
| 9 | BM 0.4 | 79.8 | 19.8 | ... | 0.4 | “ |

3.2.2 Flexural Testing. Flexural strength testing determines the resistance to flexing or how much load materials can sustain to bending. A 3-point bending test is performed on the specimen. The samples with dimensions of 127X12.5X3 mm are tested according to ASTM (D790).

3.2.3 Density Test. The density of epoxy/PLA and epoxy/PLA with nanofillers using graphene and MWCNTs is calculated based on Archimedes principle, and ASTM D79 standard is used. Using a cantilever setup and measuring unit, the actual density of each specimen is measured. The process requires the following steps: the configuration of the cantilever is placed on the weighing unit, and the weight is set to zero using the choice of tare. The sample is placed, and the weight is recorded in the air. The sample is reweighed and recorded by putting the weight in water. Then, the difference in the reading is noted and density is determined using the following equation.

$$\rho = \frac{W_{air}}{W_{air} - W_{water}}$$

where ρ = density in g/cm^3
 W_{air} = weight of specimen in air(g)
 W_{water} = weight of specimen in water(g)

4. Result and Discussion

4.1 Density Test

Density test of the prepared bio-nanocomposites is as shown in Table 8. From the results, it is observed that as reinforcement percentage of nanofillers increases, the density of the specimens increases. Density of the composite is calculated by the following equation. The higher density of the bio-composite indicates that the material has become denser and more compact as the percentage of reinforcement increases.

$$\rho_{B10} = \frac{78.75}{78.75 - 2.89} = 1.038$$

Table 8 The density of bio-composite epoxy/PLA with graphene and MWCNT

| Sl. No | Composite | Reinforcement/nanofiller, % | Density, g cm ⁻³ |
|--------|------------|-----------------------------|-----------------------------|
| 1 | Epoxy | ... | 1.1-1.2 |
| 2 | PLA | ... | 1.24 |
| 3 | Epoxy+ PLA | 10 | 1.038 |
| 4 | Epoxy+ PLA | 20 | 1.047 |
| 5 | Epoxy+ PLA | 30 | 1.048 |
| 6 | BG 0.2 | 0.2 | 1.001 |
| 7 | BG 0.3 | 0.3 | 1.025 |
| 8 | BG 0.4 | 0.4 | 1.033 |
| 9 | BM 0.2 | 0.2 | 1.049 |
| 10 | BM 0.3 | 0.3 | 1.040 |
| 11 | BM0.4 | 0.4 | 1.074 |

Table 9 Characteristic bands of composites BG0.2, BG0.3, BG0.4, BM0.2, BM0.3, and BM0.4

| BG0.2 Band, cm ⁻¹ | BG0.3 Band, cm ⁻¹ | BG0.4 Band, cm ⁻¹ | BM0.2 Band, cm ⁻¹ | BM0.3 Band, cm ⁻¹ | BM0.4 Band, cm ⁻¹ | Assignment |
|------------------------------|------------------------------|------------------------------|------------------------------|------------------------------|------------------------------|------------|
| 826 | 826 | 826 | 825 | 824 | 826 | C=C |
| 1010 | 1010 | 1010 | 1010 | 1011 | 1010 | C-O |
| 1033 | 1028 | 1034 | 1028 | 1029 | 1034 | S=O |
| 1180 | 1180 | 1180 | 1180 | 1180 | 1181 | C-O |
| 1233 | 1232 | 1237 | 1237 | 1229 | 1239 | C-O |
| 1290 | 1293 | 1295 | 1293 | 1293 | 1294 | C-O |
| 1363 | 1363 | 1359 | 1359 | 1360 | 1361 | C-H |
| 1460 | 1453 | 1456 | 1457 | 1461 | 1456 | C-H |
| 1507 | 1507 | 1507 | 1507 | 1507 | 1507 | N-O |
| 1607 | 1607 | 1606 | 1606 | 1605 | 1606 | C=C |
| 2865 | 2964 | 2871 | 2870 | 2867 | 2867 | C-H |
| 2925 | 2927 | ... | 2925 | 2926 | 2929 | C-H |
| 2961 | 2964 | 2963 | 2961 | 2959 | 2961 | C-H |

4.2 Fourier Transform Infrared Spectroscopy (FTIR)

Fourier transform infrared spectroscopy (FTIR) was based on the peak location and the frequency concerned spectral data as shown in Table 9. Epoxy resin exhibited peaks at 913 cm⁻¹ which confirms the epoxy group (Ref 43). PLA consists of lactic acid, rich in carbon chains as C=O groups, in the case of PLA—epoxy composites (Fig. 3a and b) due to carbon and hydrogen (C-H) stretching, peaks are observed at 2925 to 2929 cm⁻¹ and 2865 to 2964 cm⁻¹ which showed the stretching vibration peak of -CH₂. FTIR peaks appeared between 2959 to 2964 cm⁻¹. At 1605 to 1607 cm⁻¹, the peak is seen for the C=C stretching vibration peaks (Ref 51). 1359 cm⁻¹, 1460 and 1180 cm⁻¹ were, respectively, attributed to methyl and deformation vibration of C-H and C-O-C stretching vibration, at 1028 cm⁻¹ is the stretching vibration peak of C-O, which proved the existence of ester and difference with lactide. The peak of the epoxy group is disappeared due to the opening of the epoxy group. (Ref 52–54). The findings of this investigation shown in Fig. 3(b) indicate that spectra patterns BM0.2, BM0.3, and BM0.4 have emerged. Because of this, the underlying similarity of MWCNTs incorporated PLA/epoxy BPNCs is made up of carbon and oxygen atoms. Prominence peaks at 1605 cm⁻¹ for C=C stretching, 2925-2959 cm⁻¹ for C-H stretching, and the analysis is found to show a slight difference in intensity and transition between BM0.2 to BM0.4 BPNCs. This study stated that the absorption of carbonyl in the

PLA-Epoxy group decreased. The consequence of the study suggests that certain PLAs are associated with the epoxy & NFs because of the C-O band moved.

4.3 Thermal Analysis

TGA studies on nanofiller incorporated BPNCs are seen in Fig. 4(a) and (b). The plots demonstrate that the percentage mass of the BPNCs thermal decomposition depends on the sample temperature (BG0.2, BG0.3, BG0.4, BM0.2, BM0.3, and BM0.4) as shown in Table 10. For graphene BPNCs BG 0.2, first weight loss is observed at 171.51°C i.e., 7.313% (0.4002mg) and the second weight loss at 409.81°C 80.70% (4.416mg), respectively. BG 0.3 showed the first weight loss at 165.55°C 7.471% (0.4208mg), while the second weight loss at 406.73°C 81.76% (4.605mg) and the third weight loss occurred at 680.19°C i.e., 1.864% (0.1050mg). Similar trends were observed for BG 0.4. Compared to 0.2 and 0.3, BG 0.4 showed higher thermal degradation. Similar trends were obtained for BPNCs and BM0.4 showed higher thermal degradation.

Improved thermal degradation is observed for bio-nanocomposites reinforced with higher dosage of nanofillers.

4.4 Microstructure Analysis

The SEM micrographs of Gr and MWCNTs incorporated bio-composites are shown in Fig. 5(a)-(c) and Fig. 6(a)-(c),

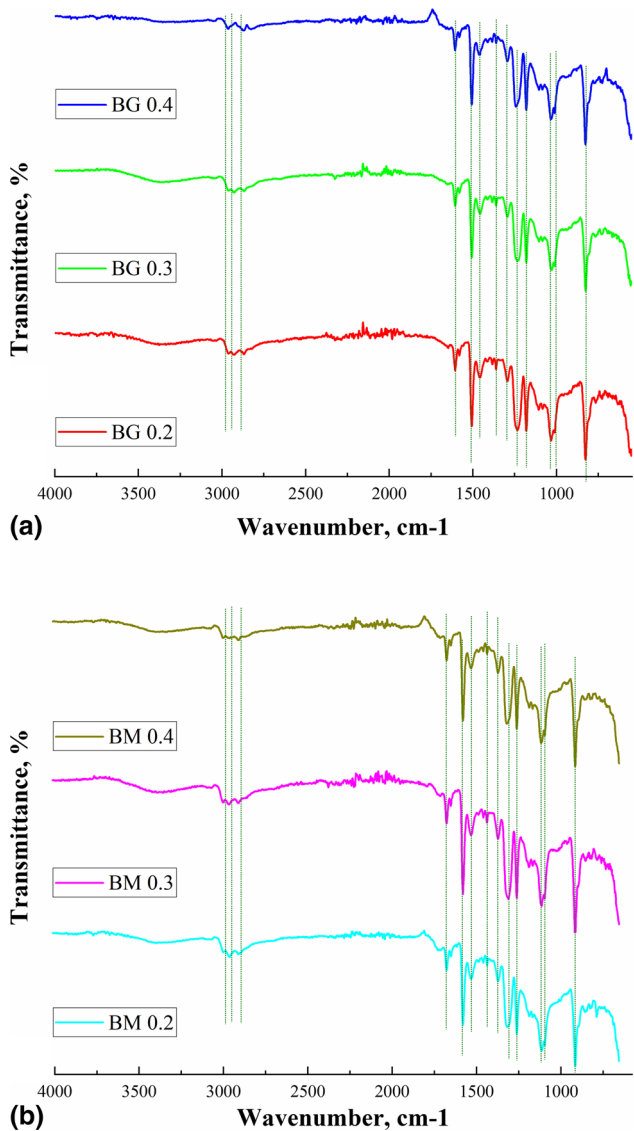


Fig. 3 FTIR spectra of bio-composites (a) BG0.2, BG0.3, BG0.4, (b) BM0.2, BM0.3, and BM0.4

respectively. Uniform dispersion of nanofillers of Gr and MWCNTs in bio-nanocomposites are analyzed using SEM micrographs. From the micrographs, it is observed that higher the wt.% of Gr and MWCNTs nanoparticles (fillers) in the polymer matrix higher is the non-uniform morphology observed.

Uniform dispersion of 0.2 wt. percent of Gr in PE resin was obtained as shown in Fig. 5. Further increase in the dosage of Gr beyond 0.2 wt.% showed agglomeration of the nanofillers used and the associated poor mechanical properties.

Similarly, uniform dispersion of 0.3 wt. percent of MWCNT in PE resin was obtained as shown in Fig. 6. The high magnification SEM micrograph in Fig. 6 clearly shows that the MWCNTs are well divided and equally embedded in the 0.2 percent PE matrix. Beyond 0.3 wt.% agglomeration of the NPs is observed. It can also be easily found that the interfacial bonding between the MWCNT and the matrix was very compact, allowing the MWCNTs to be rooted in the embedding matrix. Essentially, these MWCNTs are likely to be interlocked with polymer chains in the matrix. Thus, the inclusion of

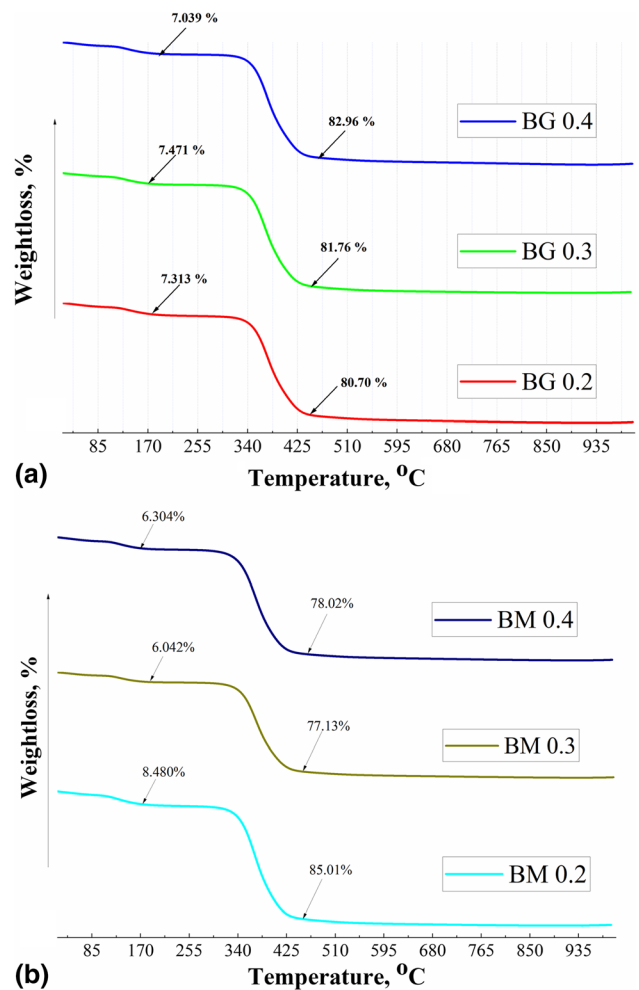


Fig. 4 TGA of bio-composites (a) BG0.2, BG0.3 and BG0.4, (b) BM0.2, BM0.3, and BM0.4

MWCNTs strengthened the crosslinking between polymer chains and increased interfacial bonding.

4.5 Mechanical Properties of Graphene-Based Hybrid Bio-Nanocomposites

The excellent properties of epoxy resins have made them one of the most widely used matrix components of polymer composites. High-performance nanocomposites can be obtained to cover a wide variety of applications by incorporating high-performance carbon fillers into epoxy resins such as graphene and MWCNTs.

The epoxy/PLA composites specimens are tested for tensile and flexural strength. The selection of B20 composite with 20% PLA was based on the previous work of the authors which stated that epoxy/PLA with 20% PLA showed improved tensile strength and decreased flexural strength (Ref 43). This optimized epoxy/PLA combination is reinforced with nanoparticles of graphene and MWCNT.

The tensile strength was carried according to ASTM D638. The tensile strength is as shown in Table 11. The stress-strain curve represented in Fig. 7 shows highest values of tensile strength, the stress-strain curve for the hybrid composites with graphene of dosage 0.2 wt.% and 0.3 wt.%. The stress-strain curves demonstrated significant nonlinearity before reaching to

Table 10 Thermal degradation of bio-composites BG0.2, BG0.3, BG0.4, BM0.2, BM0.3, and BM0.4

| | Sample code | 1st Temp, °C | | wt. in grams, mg | | 2st Temp, °C | | wt. in grams, mg | | 3rd Temp, °C | | wt. in grams, mg | |
|---|-------------|--------------|-------|------------------|--------|--------------|-------|------------------|-------|--------------|--------|------------------|--|
| | | wt. % | wt. % | wt. % | wt. % | wt. % | wt. % | wt. % | wt. % | wt. % | wt. % | | |
| 1 | BG 0.2 | 117.77 | 7.313 | 0.4002 | 345.17 | 80.70 | 4.416 | ... | ... | ... | ... | ... | |
| 2 | BG 0.3 | 171.51 | 7.471 | 0.4208 | 409.81 | 343.41 | 4.605 | 570.86 | 1.864 | 0.1050 | 680.19 | ... | |
| 3 | BG 0.4 | 166.84 | 7.039 | 0.3732 | 344.75 | 82.96 | 4.398 | ... | ... | ... | ... | ... | |
| 4 | BM 0.2 | 113.67 | 8.480 | 0.4712 | 343.66 | 85.01 | 4.724 | 613.39 | 1.377 | 0.07650 | 744.89 | ... | |
| 5 | BM 0.3 | 166.86 | 6.042 | 0.3329 | 409.08 | 343.05 | 4.250 | 576.04 | 1.877 | 0.1034 | 670.81 | ... | |
| 6 | BM 0.4 | 164.14 | 6.304 | 0.3537 | 406.24 | 341.61 | 4.377 | 576.23 | 1.922 | 0.1078 | 672.80 | ... | |
| | | 167.22 | | | 407.10 | | | | | | | | |

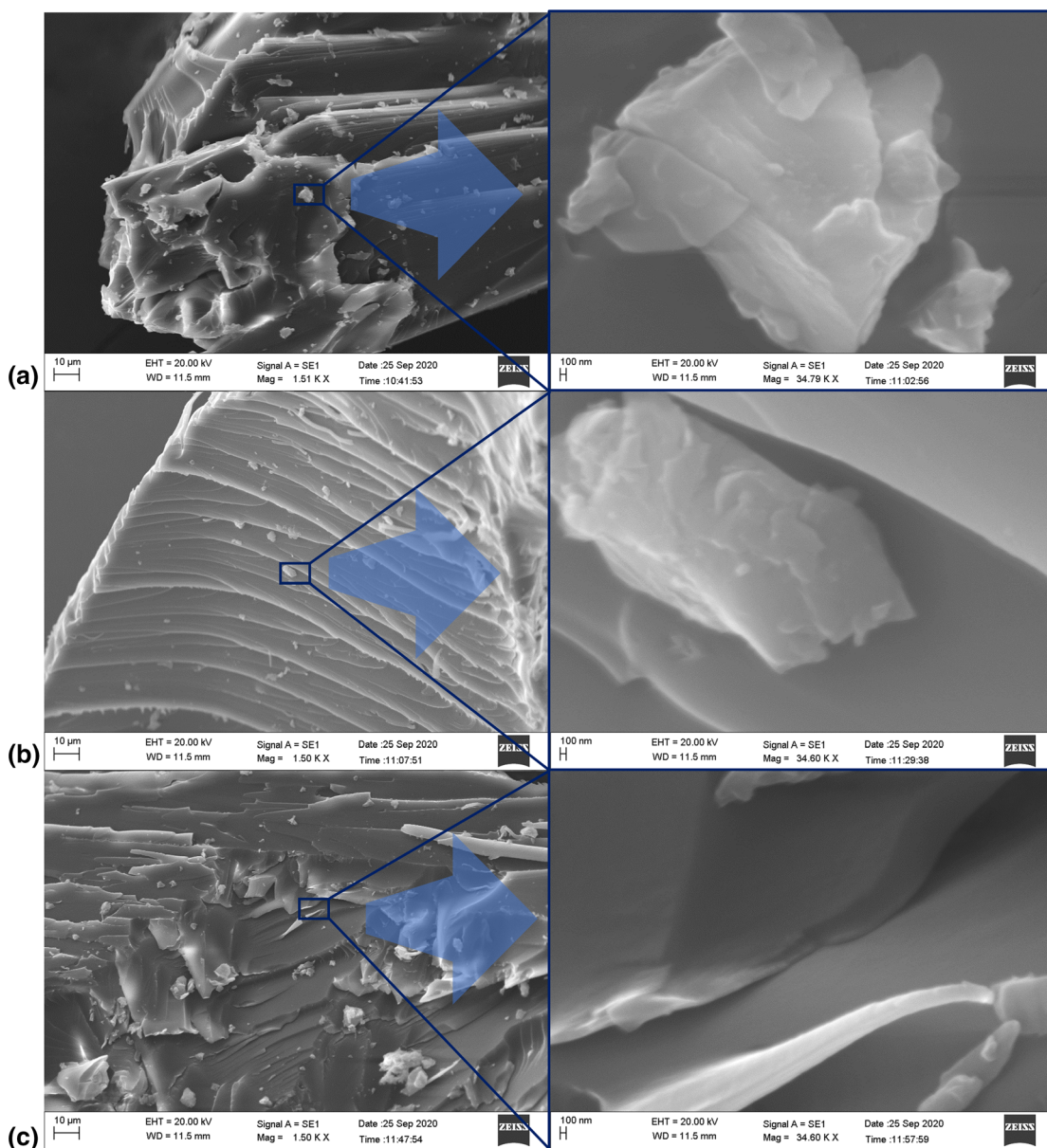


Fig. 5 SEM of bio-composites (a) BG0.2, (b) BG0.3, and (c) BG0.4

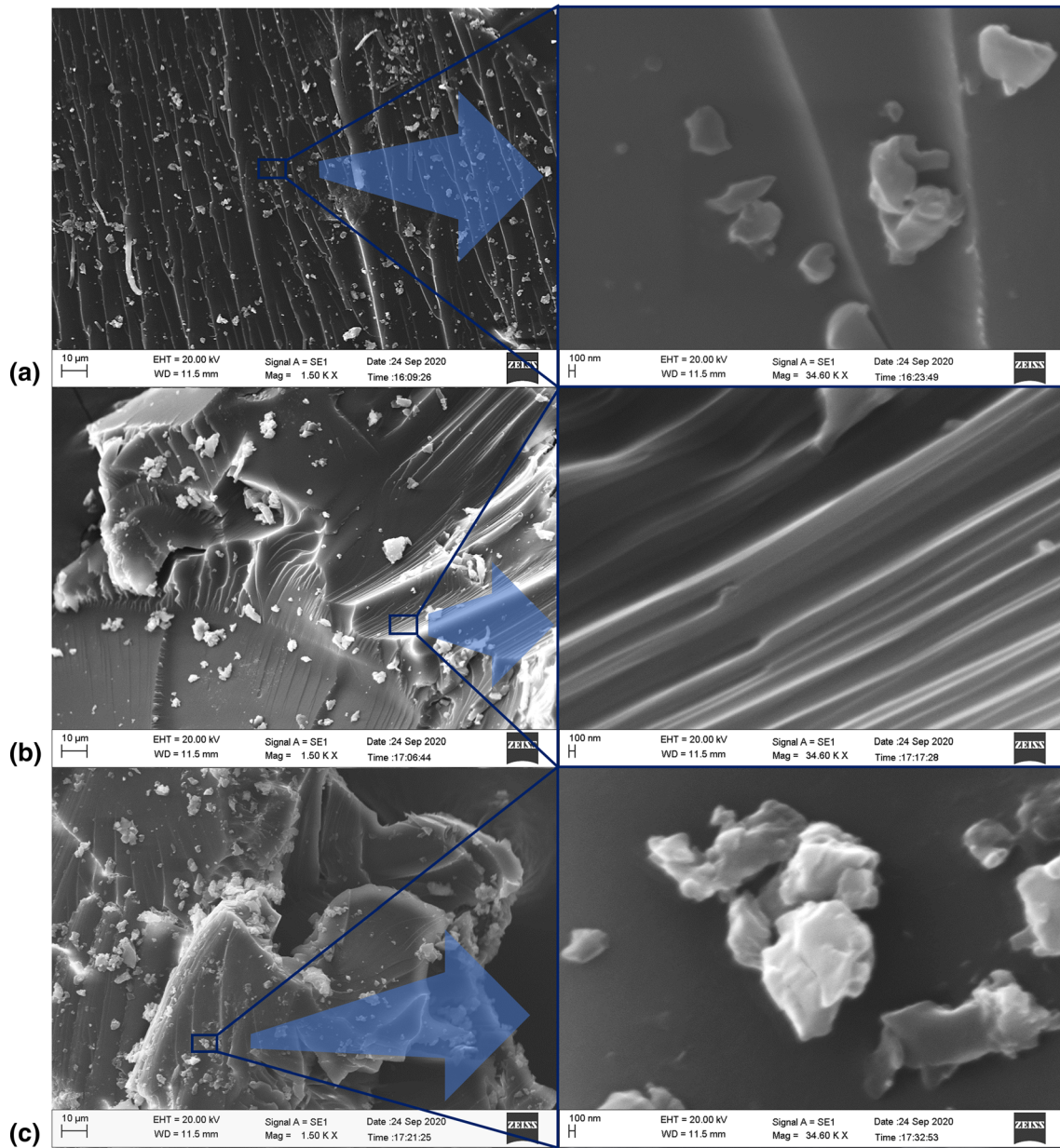


Fig. 6 SEM of bio-composites (a) BM0.2, (a) BM0.3, and (c) BM0.4

Table 11 Tensile strength of bio-nanocomposite with graphene

| Specimen | Composition | Tensile strength, MPa |
|-----------|---------------------------|-----------------------|
| Epoxy+PLA | Epoxy+PLA (20%) | 29.10 |
| BG0.2 | Epoxy+PLA+graphene (0.2%) | 28.60 |
| BG0.3 | Epoxy+PLA+graphene (0.3%) | 26.67 |
| BG0.4 | Epoxy+PLA+graphene (0.4%) | 24.27 |

breaking point, both 0.2 wt.% and 0.3 wt.% experienced lesser% of strain till breakage compared to 0.4 wt.% because of the brittleness nature of the composites.

Figure 8 shows average tensile strength, and it is found as 28.6 and 26.67 MPa, for 0.2 Wt.%, 0.3 Wt.%, respectively. High strength of the hybrid composite is due to the crystallinity

of the biopolymer, which increases strength as in the crystalline phase, and the intermolecular bonding and interfacial interaction is more significant. This can be evidenced from SEM images of BPNCs. Simultaneously, stress–strain curve of graphene with 0.4% showed higher% of strain at breakage compared to its 0.2 and 0.3wt.% dosage. The hybrid nanocom-

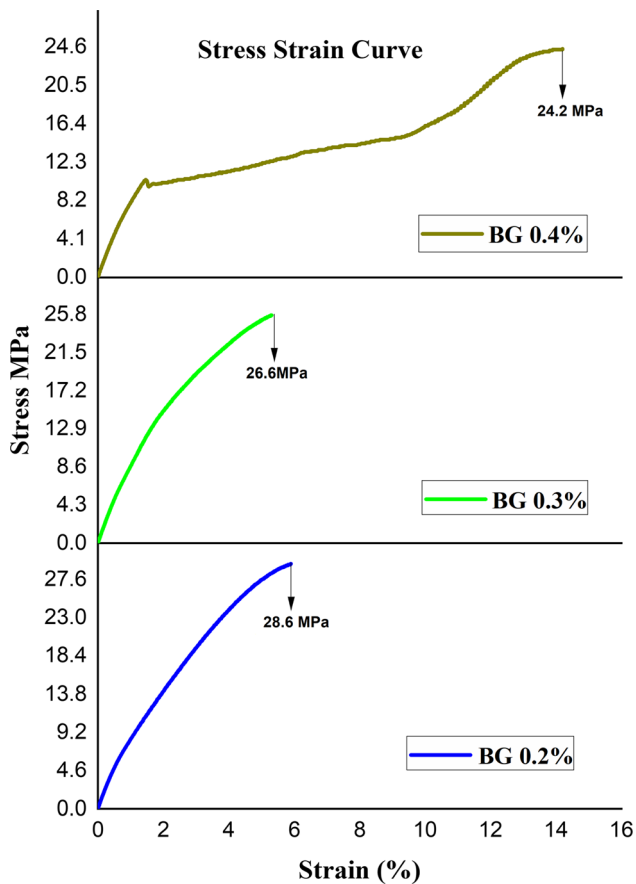


Fig. 7 Stress-strain curve for varied percentage of graphene nanoparticles

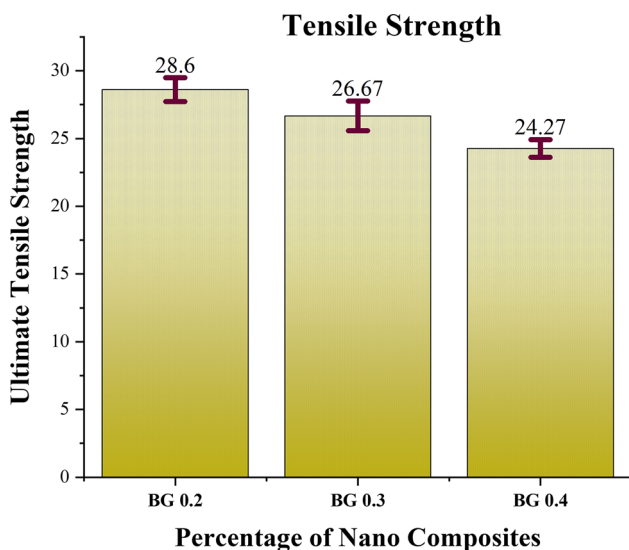


Fig. 8 Tensile strength for varied percentage of graphene nanoparticles

posite has become more elastic as the percentage of nanofillers increased. Composite showed a lower strength tensile strength of 24.27MPa for higher dosage (0.4 wt.%). This is because the composite can be severely compromised by inadequate filler-matrix adhesion at the interface, and fillers may not serve as replacements and provide defects in the matrix. Hence tensile

strength decreased by 1.74% compared to a pristine sample of Epoxy/PLA. Similar kinds of results are reported in the literature (Ref 55–57).

4.6 Flexural Strength

Flexural strength test findings of hybrid nanocomposite are shown in Table 12. Flexural strength decreased drastically as the percentage reinforcement of nanofillers of graphene and MWCNTs increases. Graphene with 0.2 wt% shows a higher flexural strength of 143.67 MPa, whereas graphene with 0.3 and 0.4 wt% shows 82.4 and 91.00 MPa, respectively (Fig. 9). The explanation for the decrease in flexicity of hybrid composites is due to the presence of voids which reduce the flexicity of composites consisting of nanoparticles, and they act as centers of concentration of tension. An agglomeration of the particles is the primary reasons for the creation of these voids. Hence, the Flexural strength of 0.2wt.% shows an improvement by 177.89% compared to pristine sample of epoxy/PLA composites.

4.7 Mechanical Properties of MWCNTs

Figure 10 shows the stress-strain curve of a hybrid nanocomposite reinforced with MWCNTs, which demonstrates the highest tensile strength values and shows nonlinear behaviour before breaking. The hybrid composites with 0.2 and 0.3 wt% experienced lesser% strain because of the brittle nature of the hybrid nanocomposites compared to 0.4wt%. The result showed that tensile strength increases until 0.3%, beyond which it decreases as the percentage of reinforcement increases and the hybrid bio-nanocomposites exhibit reduced deformation. The maximum tensile strength of 21.13 MPa at 0.3 wt.% of MWCNT is shown in Table 13, and it is depicted in Fig. 11 which shows average values of tensile strength. The interfacial interaction between the hybrid composites consisting of epoxy/PLA chain MWCNT as evidenced by homogenous dispersion of nanofillers seen in the SEM images. Reduced tensile strength for 0.4wt.% MWCNT is observed at 15.92 MPa; the reason for reduced tensile strength is due to agglomeration of the nanoparticles used. It can be seen from the graph that elongation at break increases with an increase in MWCNT percentage. Composites with 0.4 wt.% MWCNT experienced maximum elongation at break, which indicates that the composite experienced higher deformation; this may be due to weak adhesion of the filler matrix at the interface, which weakens the hybrid bio-nanocomposites. The tensile strength of hybrid bio-nanocomposite is decreased by 26.80% compared to the pristine sample of epoxy/PLA.

4.8 Flexural Strength

Flexural strength studies showed in Table 14 that it is maximum –75.83 MPa for 0.2 wt.% of MWCNT, and decreases as the% of the reinforcement increases, as shown in Fig. 12. The increase in flexural strength at 0.2wt% is due to interfacial adhesion between nanofillers and the matrix. Higher percentage MWCNT reduced the flexural strength, and is due to the polymer molecule attracted by the high surface area of nanoparticles and thus decreases the mobility of polymer chains, leading to an increase in viscosity in the polymer matrix and a further decrease in the load-carrying ability of CNTs; local stresses are produced by an increase in the viscosity of the matrix.

Table 12 Flexural strength of bio-nanocomposite with graphene

| Specimen | Composition | Flexural strength, MPa |
|-----------|---------------------------|------------------------|
| Epoxy+PLA | Epoxy+PLA(20%) | 51.70 |
| BG0.2 | Epoxy+PLA+graphene (0.2%) | 143.67 |
| BG0.3 | Epoxy+PLA+graphene (0.3%) | 82.40 |
| BG0.4 | Epoxy+PLA+graphene (0.4%) | 91.00 |

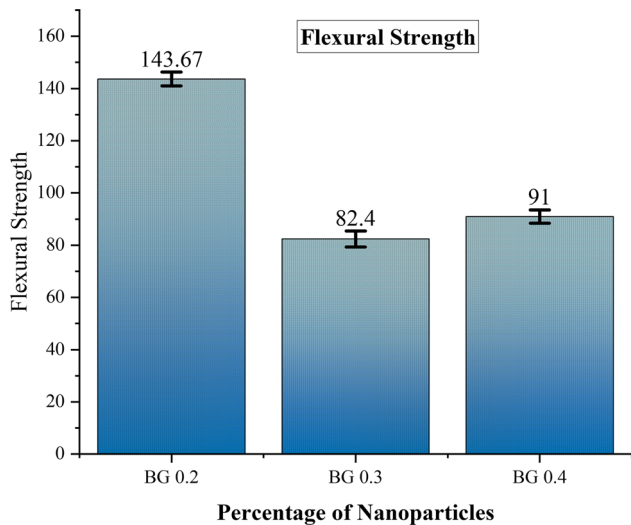


Fig. 9 Flexural strength for varied percentage of graphene nanoparticles

From the mechanical characterization analysis of the BPNCs carried out, it is found that graphene with 0.2 wt.% showed higher tensile strength by 25.52% compared to MWCNT.

4.9 Mechanical Strength Mechanism of NFs (Gr and MWCNT)-Incorporated Biopolymer Composites

This section highlights on the mechanism of deformation of polymer chains observed in the BPNCs synthesized. Figure 13 demonstrates the potential deformation mechanism of the NFs (Gr and MWCNT) embedded in BPNCs. Generally, the polymers are of amorphous and semi-crystalline in nature. Epoxy has more brittleness owing to the large number of crystalline properties at the molecular level, in comparison to PLA. Addition of the NFs enhances its semi-crystalline properties due to this brittleness decreases, and the ductility increases as a result of the composite that can tolerate higher degrees of deformation. Figure 13 exhibits amorphous region of BPNCs showing poorer bonds when compared to semi-crystalline and crystalline regions owing to a reduced number of NFs bonds. Despite a relatively high degree of comprehension of biopolymer nanocomposite (BPNC), mechanical reinforcement pathway with Grs and MWCNTs provides remarkable mechanical properties of both NFs in BPNC. However, the mechanisms have not yet been thoroughly understood by researchers. Development of Gr and MWCNTs-reinforced epoxy/PLA combination could provide a viable solution as both nanofillers used can provide multi-functional properties together with improved efficiency at very low wt.% of their dosage. The main objective of the work is to

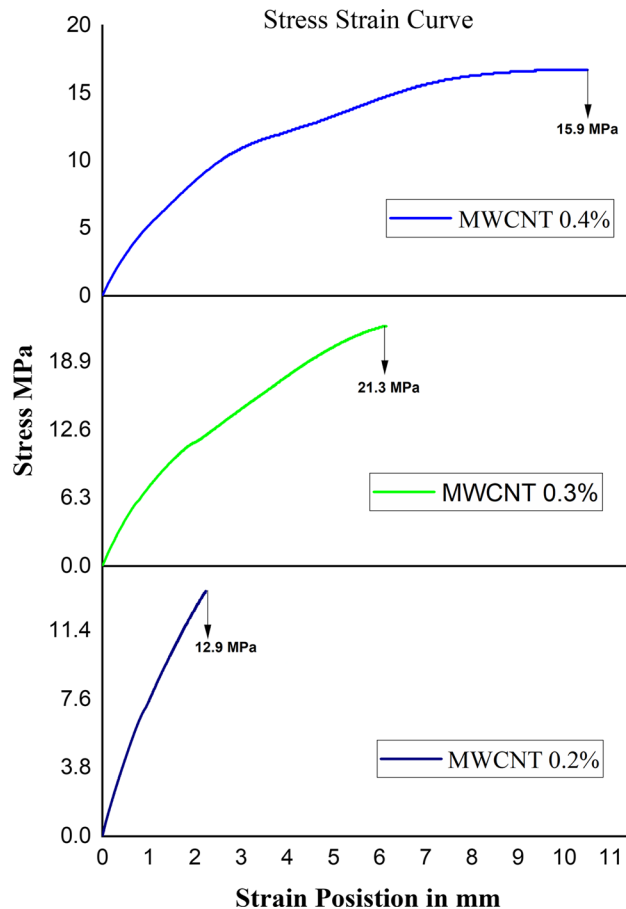


Fig. 10 Stress-strain curve for varied percentage of MWCNT

obtain higher efficiency of the BPNCs composites developed which can be scaled up to industrial level, thereby replacing the conventional materials, and take advantage of the superior properties of these novel materials.

Figure 14 shows the statistical analysis of the experimental data of tensile and flexural strength of hybrid bio-nanocomposites, in accordance with Fig. 8, 9, 11 And 12 and Tables 11, 12, 13, 14 the relations between flexural and ultimate tensile strengths of BM and BG series with their different concentration average variations, compared plotted graph in Fig. 14. It will give detailed comparative analysis of strengths of both BM and BG series. An increase in the percentage of nanofillers in the matrix leads to a decrease in their flexural strength of BM series and ultimate tensile strengths of BG series. This indicates that 0.2 wt.% is having high strength in both series. Similarly, in the case of the flexural strength of BG series and ultimate tensile strengths of BM series shown polynomial variation (with degree of coefficient 1). Individual, in flexural strength of

BG 0.2 wt.% whereas 0.3% in ultimate tensile strengths showed higher value. Overall comparison, it indicates that 0.2 wt.% showed higher flexural strength in both series and at 0.3 wt.% in BM and 0.2 wt.% in BG series showed the improved tensile strength. The flexural and ultimate tensile strengths variation can be carried out by varying percentage of nanofillers based on their required applications.

5. Simulation Method

The era has changed from conventional methods of work to virtual methods, in particular simulation has come a long way to completely skip the process of physical prototype building (Ref 58). As the process led to drastic time and cost reduction, which is the current need for any domain. However, simulation

Table 13 Tensile strength of bio-nanocomposite with MWCNT

| Specimen | Composition | Tensile strength, MPa |
|-----------|--------------------------|-----------------------|
| Epoxy+PLA | Epoxy+PLA (20%) | 29.10 |
| BM 0.2 | Epoxy+PLA+MWCNT (0.2%) | 12.93 |
| BM 0.3 | Epoxy+ PLA+ MWCNT (0.3%) | 21.3 |
| BM 0.4 | Epoxy+PLA+MWCNT (0.4%) | 15.92 |

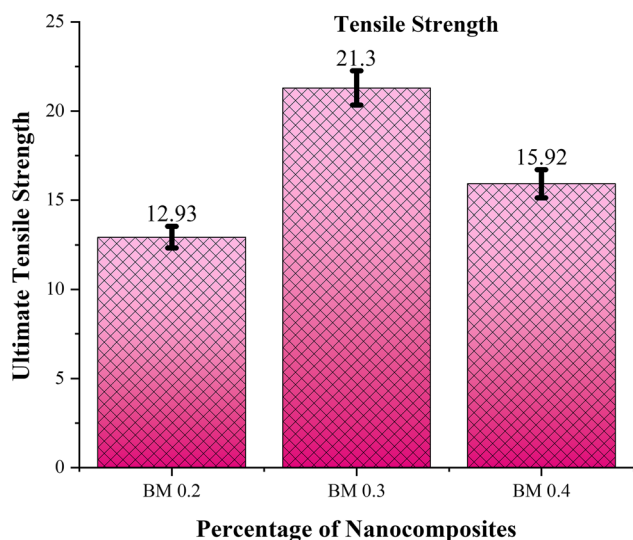


Fig. 11 Tensile strength for varied percentage of MWCNT

has still to cover a long distance to replace the physical model (Ref 59). In this regard, lot many modifications are happening in the stream of industry internet of things. In particular, mechanical software tools able to take a big leap in reducing the error percentage by working on the software programming aspects (Ref 60). The current work has some features of the same, which were discussed in detail.

5.1 Geometry

The solid model of the coupon built in design modeler as per ASTM 7264M for flexural strength test (Ref 61) as depicted in Fig. 15. The coupon comprising three layers like laminates, top and bottom layer made out of epoxy resin and the middle layer is of polylactic acid (Ref 62). The composition is in the range of 10 to 50% in steps of 10 per condition.

5.2 Contact Generation

Contact generation happens when more than one component assembled together. The entire coupon resembling the physical model subjected to a bonding with epoxy to PLA, which is of the form 'permanant joint' or 'bonded joint' (Ref 63) as mentioned in Fig. 16, 17.

5.3 Mesh Generation

Discretization process is a common phenomenon in finite element analysis. For the coupon Solid 186 with 20 noded hexa-dominant element (Ref 39) is considered. The element

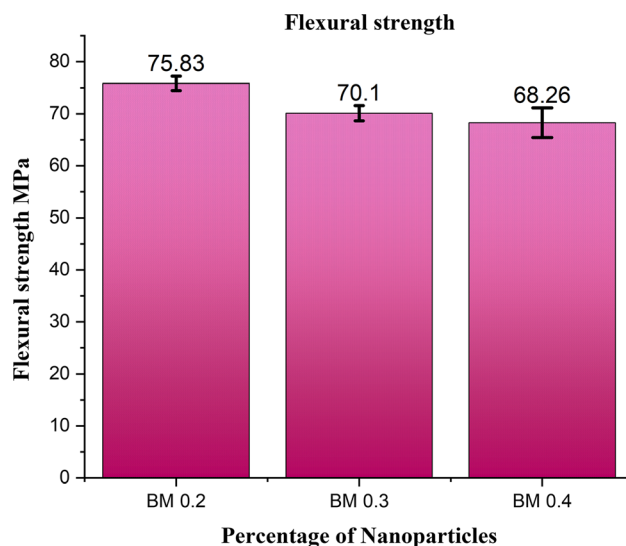


Fig. 12 Flexural strength for varied percentage of MWCNT

Table 14 Flexural strength of bio-composite with MWCNT

| Specimen | Composition | Flexural strength, MPa |
|-----------|------------------------|------------------------|
| Epoxy+PLA | Epoxy+PLA (20%) | 51.70 |
| BM 0.2 | Epoxy+PLA+MWCNT (0.2%) | 75.83 |
| BM 0.3 | Epoxy+PLA+MWCNT (0.3%) | 70.10 |
| BM 0.4 | Epoxy+PLA+MWCNT (0.4%) | 68.26 |

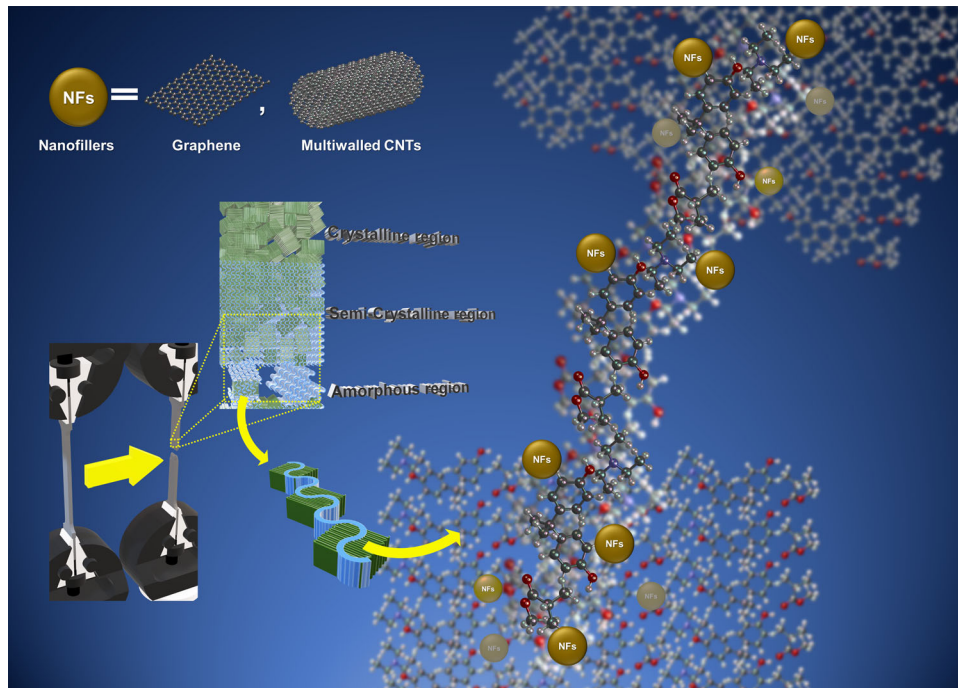


Fig. 13 Schematic diagram explaining the proposed pathway of mechanical strength mechanism of NFs (Gr and MWCNT) incorporated biopolymer composites

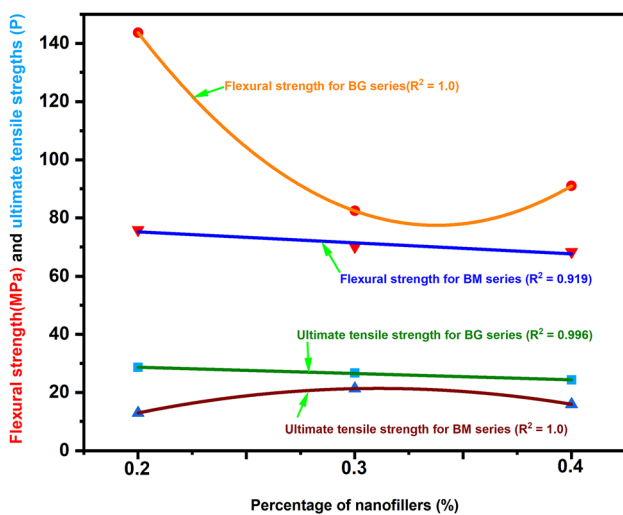


Fig. 14 A comparison of flexural and tensile strengths of BM and BG series with their different weight percentages of nanofillers

type has second order element, preferred for better accuracy. The convergence criteria have been met with both H-Type and P-Type method implementation into the model.

5.4 Loads and Boundary conditions

The coupons are subjected to a load capacity as specified in experimental condition. There are two ways to solve for virtual analysis (Ref 49), firstly considering the yield limit or ultimate limit as the threshold value for solving the problem or to choose the experimental value-based analysis. As the support element

is considered as fixed in all degrees of freedom (instead it should be roller supported—due to infinite stress condition or rigid body motion). Further the details of load and boundary condition are shown in Fig. 18.

5.5 Total Deformation

One typical case of 20% inclusion of PLA is considered in epoxy resin for demonstration of virtual analysis. The value of 2.65 mm is observed for the composition as shown in Fig. 19.

5.6 Von Mises Stress

The analysis as shown in Fig. 20 illustrates about 73.24 MPa of stress which is above than the threshold limit of PLA and epoxy resin combination together.

5.7 Reinforcement of MWCNT and Graphene

The simulation is incomplete without nanoparticles embedded in PLA and epoxy based substrate. The model in simulation is considered assuming few parameters such as Graphene being analyzed as circular tube like structure. The geometrical model as shown in Fig 21 indicates reinforcement of graphene in epoxy-PLA substrate. Figure 22 illustrates the contact generation between graphene and PLA using 'Bonded' contact. Mesh generation is depicted in Fig. 23.

Figure 24 infers the total deformation showing 851 μ m (.851mm) and stress value is 51.1 MPa as shown in Fig. 25. This is comparatively lower than that of the epoxy and PLA substrate (73.246MPa).

5.8 Comparative Study

The entire work of experimental and numerical analysis is based on the assumption that -

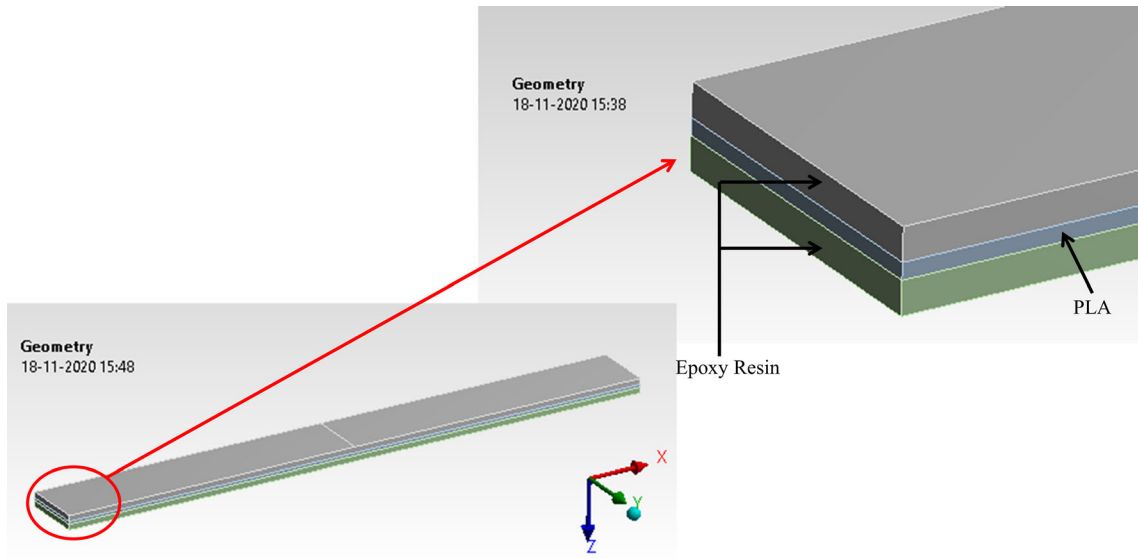


Fig. 15 Solid model of coupon built in design modeler

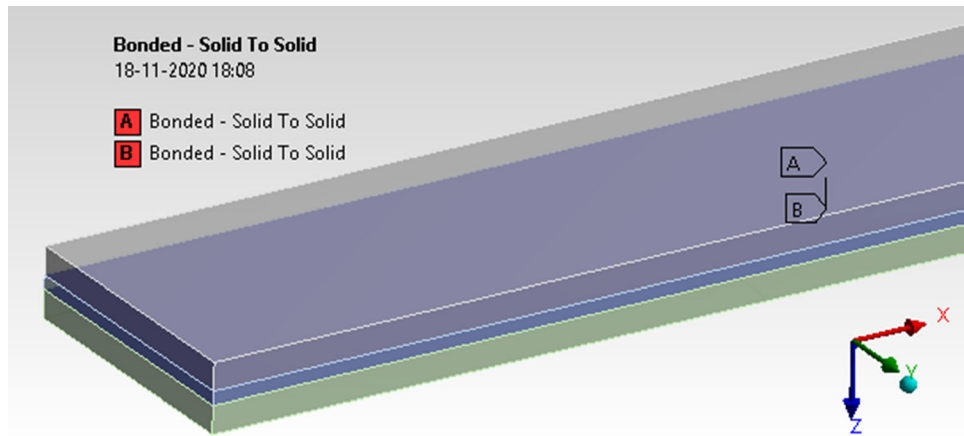


Fig. 16 Contact generation

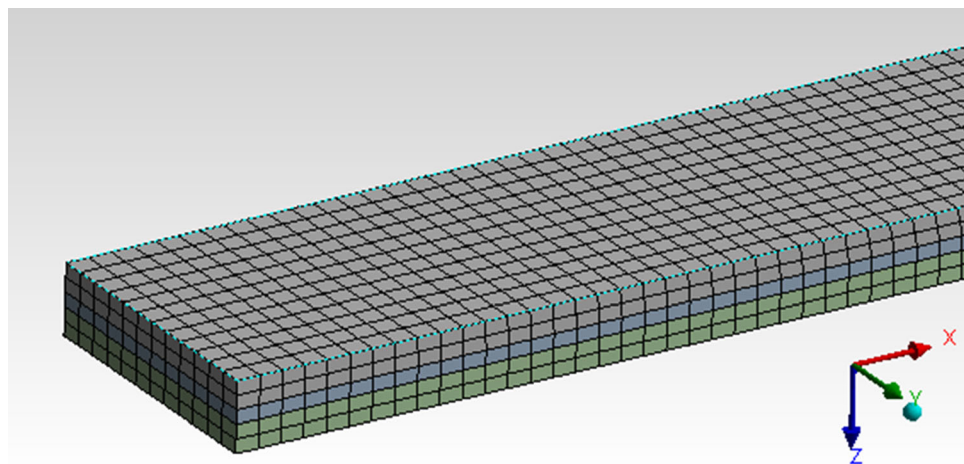


Fig. 17 Mesh generation

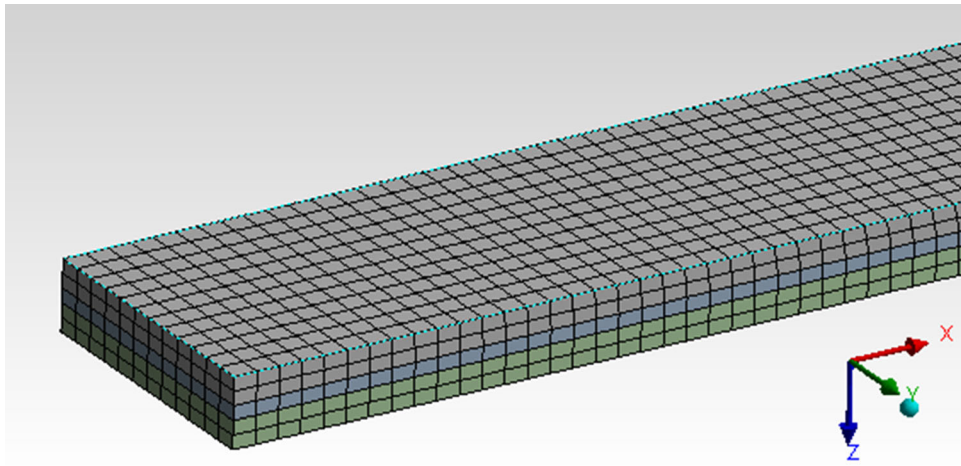


Fig. 18 Loads and boundary conditions

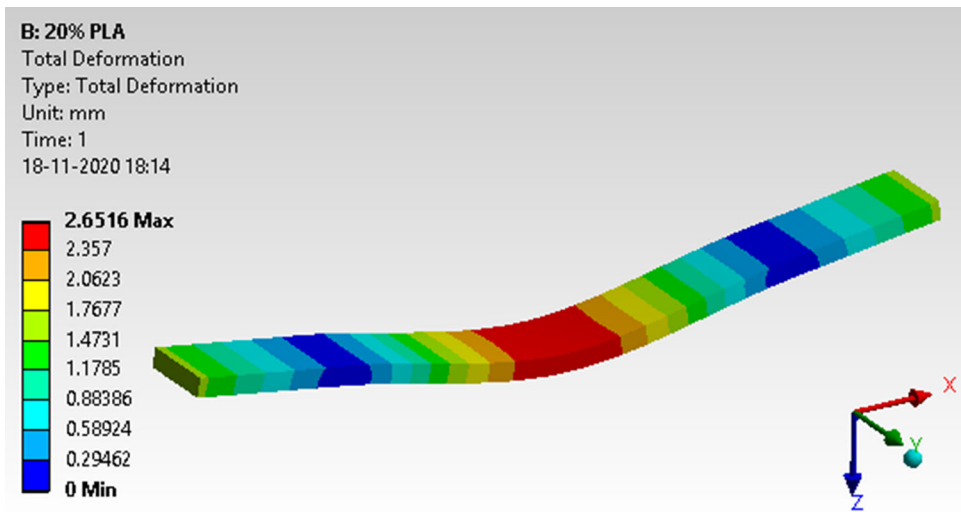


Fig. 19 Total deformation

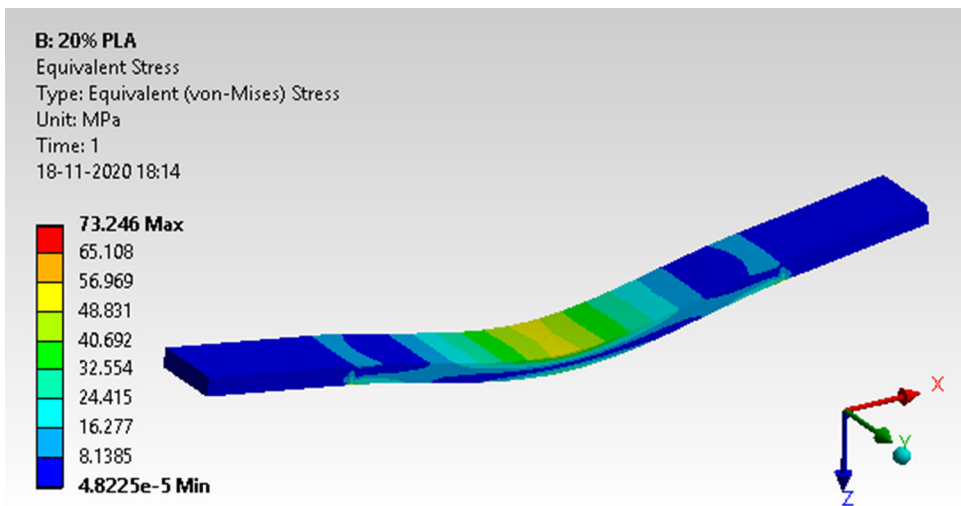


Fig. 20 Von Mises stress

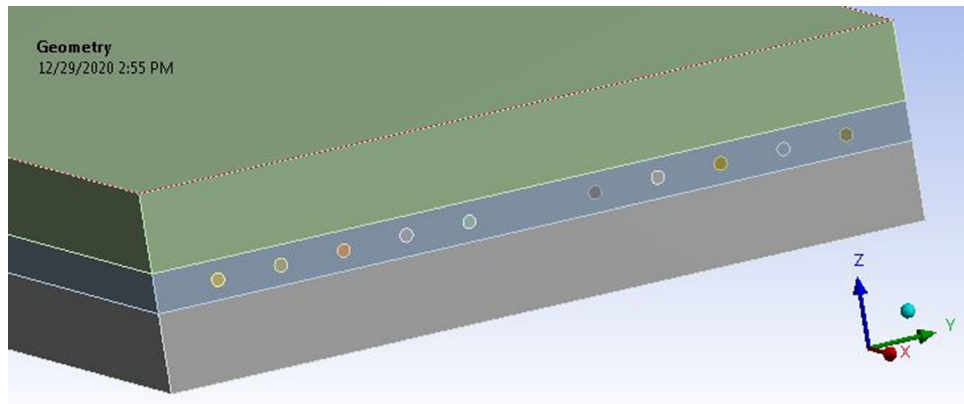


Fig. 21 Geometry with graphene reinforcement

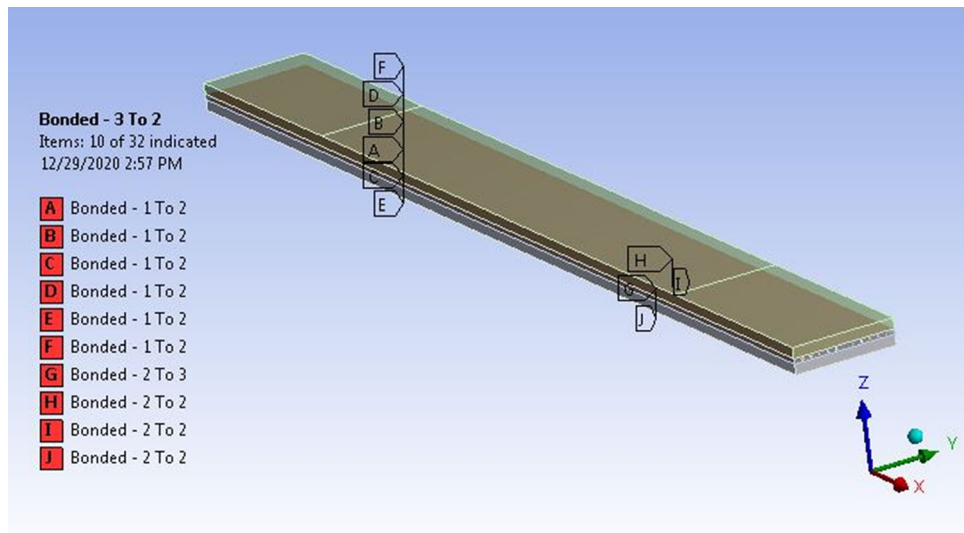


Fig. 22 Contact generation between graphene and PLA/epoxy resin

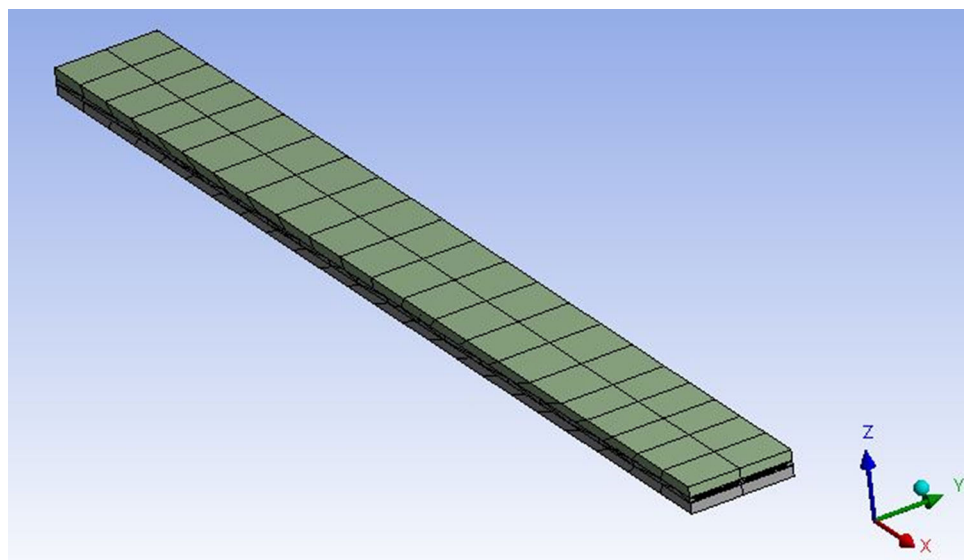


Fig. 23 Mesh generation

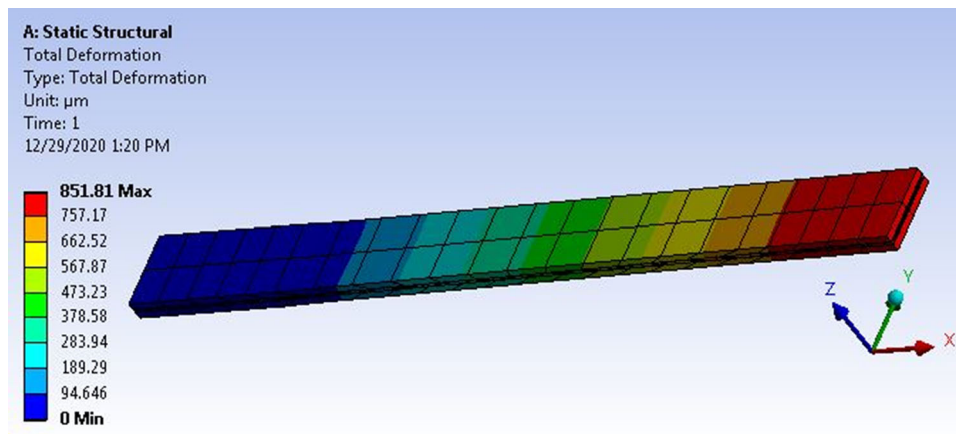


Fig. 24 Total deformation

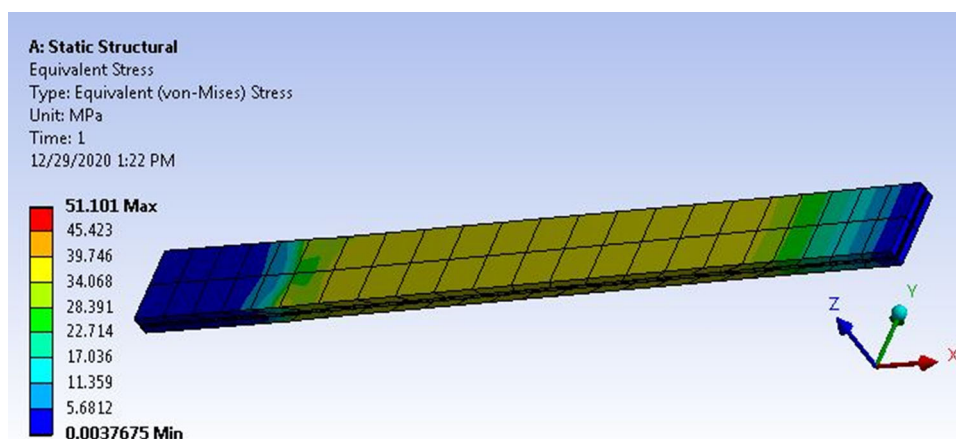


Fig. 25 Von Mises stress

- The composition is uniform across the length without any agglomeration of material.
- An error percentage of less than or equal to 20 is acceptable due to more than one composition mixed at varied percentage (Ref 64).

The composition can be considered for volume/weight fraction depending on the experimental work, as the same has to be utilized for numerical condition

6. Conclusions

From the exhaustive work carried out on the feasibility studies of hybrid bio-nanocomposites for automotive component applications, the following conclusions are drawn. Use of PLA as biopolymer for the synthesis of nanocomposites reduces dependency on synthetic polymer partially. 0.2wt.% graphene reinforced in biopolymer showed a decrease in tensile strength by 1.74% and an increase in flexural strength by

177.89% compared to 20 wt.% epoxy with PLA (Ref 43), while 0.3wt.% of MWCNT showed a decrease in tensile strength by 26.80% compared to epoxy/PLA (Ref 43). However, the flexural strength of 0.2 wt.% of MWCNT increased by 31.82% compared to epoxy/PLA (Ref 43). Microstructural studies of synthesized BPNCs by SEM micrographs showed uniform distribution of the NFs for lower dosage. Beyond 0.3 wt.% of both nanofillers showed the agglomeration of the NFs in the holding matrix. TGA showed improved thermal degradation for higher dosage of the NFs in the holding matrix and the bonding between matrix and filler is confirmed by FTIR studies. FEA analysis showed close agreement with the experimental results of mechanical properties of the synthesized BPNCs.

References

1. N.H. Mostafa, Z. Ismarrubie, S. Sapuan and M. Sultan, Fibre Prestressed Polymer-Matrix Composites: A Review, *J. Compos. Mater.*, 2017, 51(1), p 39–66

2. L. Botta, R. Scaffaro, F. Suter and M.C. Mistretta, Reprocessing of PLA/Graphene Nanoplatelets Nanocomposites, *Polymers*, 2018, **10**(1), p 18
3. R. Xiong, A.M. Grant, R. Ma, S. Zhang and V.V. Tsukruk, Naturally-Derived Biopolymer Nanocomposites: Interfacial Design, Properties and Emerging Applications, *Mater. Sci. Eng. R. Rep.*, 2018, **125**, p 1–41
4. A. Dadkhah Tehrani and M. Parsamanesh, Preparation, Characterization and Drug Delivery Study of a Novel Nanobiopolymeric Multidrug Delivery System, *Mater. Sci. Eng. C*, 2017, **73**, p 516–524
5. P. Feng, Y. Kong, L. Yu, Y. Li, C. Gao, S. Peng, H. Pan, Z. Zhao and C. Shuai, Molybdenum Disulfide Nanosheets Embedded with Nanodiamond Particles: Co-Dispersion Nanostructures as Reinforcements for Polymer Scaffolds, *Appl. Mater. Today*, 2019, **17**, p 216–226
6. C. Shuai, W. Guo, P. Wu, W. Yang, S. Hu, Y. Xia and P. Feng, A Graphene Oxide-Ag Co-Dispersing Nanosystem: Dual Synergistic Effects on Antibacterial Activities and Mechanical Properties of Polymer Scaffolds, *Chem. Eng. J.*, 2018, **347**, p 322–333
7. C. Shuai, W. Yang, P. Feng, S. Peng and H. Pan, Accelerated Degradation of HAP/PLLA Bone Scaffold by PGA Blending Facilitates Bioactivity and Osteoconductivity, *Bioact. Mater.*, 2021, **6**(2), p 490–502
8. C. Salom, M.G. Prolongo, A. Toribio, A.J. Martínez-Martínez, I.A. de Cárcer and S.G. Prolongo, Mechanical Properties and Adhesive Behavior of Epoxy-Graphene Nanocomposites, *Int. J. Adhes. Adhes.*, 2017, **2018**(84), p 119–125
9. J. Cha, J. Kim, S. Ryu and S.H. Hong, Comparison to Mechanical Properties of Epoxy Nanocomposites Reinforced by Functionalized Carbon Nanotubes and Graphene Nanoplatelets, *Compos. Part B: Eng.*, 2019, **162**, p 283–288
10. A. Kumar, K. Sharma and A.R. Dixit, A Review of the Mechanical and Thermal Properties of Graphene and Its Hybrid Polymer Nanocomposites for Structural Applications, *J. Mater. Sci.*, 2019, **8**, p 5992–6026
11. D. Yao, N. Peng and Y. Zheng, Enhanced Mechanical and Thermal Performances of Epoxy Resin by Oriented Solvent-Free Graphene/Carbon Nanotube/Fe₃O₄ Composite Nanofluid, *Compos. Sci. Technol.*, 2018, **167**, p 234–242
12. D.J. Thomas, Developing Hybrid Carbon Nanotube- and Graphene-Enhanced Nanocomposite Resins for the Space Launch System, *Int. J. Adv. Manuf. Technol.*, 2020, **110**(7–8), p 2249–2255
13. N.H. Mostafa, Z.N. Ismarubie, S.M. Sapuan and M.T.H. Sultan, Fibre Prestressed Composites: Theoretical and Numerical Modelling of Unidirectional and Plain-Weave Fibre Reinforcement Forms, *Compos. Struct.*, 2017, **159**, p 410–423
14. M.J. Sharba, Z. Leman, M.T.H. Sultan, M.R. Ishak and M.A.A. Hanim, Tensile and Compressive Properties of Woven Kenaf/Glass Sandwich Hybrid Composites, *Int. J. Polym. Sci.*, 2016, **2016**, p e1235048
15. S.D. Salman, Z. Leman, M. Ishak, M. Sultan and F. Cardona, Quasi-Static Penetration Behavior of Plain Woven Kenaf/Aramid Reinforced Polyvinyl Butyral Hybrid Laminates, *J. Ind. Text.*, 2018, **47**(7), p 1427–1446
16. S. Suresh, P. Nisha, P. Saravanan, K. Jayamoorthy and S. Karthikeyan, Investigation of the Thermal and Dielectric Behavior of Epoxy Nano-Hybrids by Using Silane Modified Nano-ZnO, *Silicon*, 2018, **10**(4), p 1291–1303
17. S. Parbin, N.K. Waghmare, S.K. Singh and S. Khan, Mechanical Properties of Natural Fiber Reinforced Epoxy Composites: A Review, *Procedia Comput. Sci.*, 2019, **152**, p 375–379
18. E. Sarikaya, H. Çallioğlu and H. Demirel, Production of Epoxy Composites Reinforced by Different Natural Fibers and Their Mechanical Properties, *Compos. B Eng.*, 2019, **167**(15), p 461–466
19. S.A. Hallad, N.R. Banapurmath, V. Patil, V.S. Ajarekar, A. Patil, M.T. Godi and A.S. Shettar, Graphene Reinforced Natural Fiber Nanocomposites for Structural Applications, *IOP Conf. Ser.: Mater. Sci. Eng.*, 2018, **376**, p 012072
20. H.K. Madhusudhana, K. Ruhi, R.L. Anand and C.S. Venkatesha, Experimental Study on Fracture Toughness of Natural Fibres Reinforced Hybrid Composites, *IOP Conf. Ser.: Mater. Sci. Eng.*, 2018, **376**, p 012088
21. H.K. Madhusudhana, B. Desai and C. Venkatesha, Experimental Investigation on Parameter Effects on Fracture Toughness of Hemp Fiber Reinforced Polymer Composites, *Mater. Today: Proc.*, 2018, **5**(9), p 20002–20012
22. H.K. Madhusudhana, G.J. Satish, N. Vijayakumar and P. Sachin, Design and Optimization of Operating Parameters for Areca Nut De-Husker, *IOP Conf. Ser.: Mater. Sci. Eng.*, 2020, **872**, p 012011
23. A.Y. Patil, N.U. Hrishikesh, G.D. Basavaraj, G.R. Chalageri and K.G. Kodancha, Influence of Bio-Degradable Natural Fiber Embedded in Polymer Matrix, *Mater. Today: Proc.*, 2018, **5**(2), p 7532–7540
24. P.A. Prasob and M. Sasikumar, Static and Dynamic Behavior of Jute/Epoxy Composites with ZnO and TiO₂ Fillers at Different Temperature Conditions, *Polymer Testing*, 2018, **69**, p 52–62
25. S. Suchat, A. Lanna, A. Chotikhun and S. Hiziroglu, Some Properties of Composite Drone Blades Made from Nanosilica Added Epoxidized Natural Rubber, *Polymers*, 2020, **12**(6), p 1293
26. K. Leelachai, P. Kongkachuichay and P. Dittanet, Toughening of Epoxy Hybrid Nanocomposites Modified with Silica Nanoparticles and Epoxidized Natural Rubber, *J. Polym. Res.*, 2017 <https://doi.org/10.1007/s10965-017-1202-y>
27. L. Guadagno, M. Raimondo, V. Vittoria, L. Vertuccio, C. Naddeo, S. Russo, B. De Vivo, P. Lamberti, G. Spinelli and V. Tucci, Development of Epoxy Mixtures for Application in Aeronautics and Aerospace, *RSC Adv.*, 2014, **4**(30), p 15474–15488
28. J. Joy, E. George, S. Thomas and S. Anas, Effect of Filler Loading on Polymer Chain Confinement and Thermomechanical Properties of Epoxy/Boron Nitride (h-BN) Nanocomposites, *New J. Chem.*, 2020, **44**(11), p 4494–4503
29. A.M. Sajjan, N.R. Banapurmath, N.M. Shivayyanavar, A.S. Kulkarni and A.S. Shettar, Development and Characterization of Silicon Carbide Incorporated Graphene Amine-Based Polymer Nanocomposites for Structural Applications, *IOP Conf. Ser.: Mater. Sci. Eng.*, 2018, **376**(1), p 012073
30. S. Nath, H. Jena and D. Sahini, Analysis of Mechanical Properties of Jute Epoxy Composite with Cenosphere Filler, *Silicon*, 2019, **11**(2), p 659–671
31. A.M.N. Azammi, S.M. Sapuan, M.R. Ishak and M.T.H. Sultan, Conceptual Design of Automobile Engine Rubber Mounting Composite Using TRIZ-Morphological Chart-Analytic Network Process Technique, *Def. Technol.*, 2018, **14**(4), p 268–277
32. N.H. Mostafa, Z. Ismarubie, S. Sapuan and M. Sultan, Effect of Equi-Biaxially Fabric Prestressing on the Tensile Performance of Woven E-Glass/Polyester Reinforced Composites, *J. Reinf. Plast. Compos.*, 2016, **35**(14), p 1093–1103
33. M.T.H. Sultan, K. Worden, W.J. Staszewski, S.G. Pierce, J.M. Dulieu-Barton, and A. Hodzic, Impact Damage Detection and Quantification in CFRP Laminates; a Precursor to Machine Learning. 2009, <https://prints.soton.ac.uk/71820/>. Accessed 24 March 2021
34. Y. Zhou, L. Lei, B. Yang, J. Li and J. Ren, Preparation and Characterization of Poly(lactic Acid) (PLA) Carbon Nanotube Nanocomposites, *Polym. Testing*, 2018, **68**, p 34–38
35. A.V. Rane, K. Kanny, A. Mathew, M.T. Pandurangan and S. Thomas, Microstructural Features Affecting Mechanical Properties: Effect of Processing on Dispersion of Carbon Black (N220) Nanoparticles Reinforcement in Poly (Lactic Acid), *Surf. Interfaces*, 2020, **18**(January), p 100451
36. F. Hedayati, N. Moshiri-Gomchi, M. Assaran-Ghomi, S. Sabahi, N. Bahri-Laleh, S. Mehdipour-Ataei, J. Mokhtari-Aliabad and S.A. Mirmohammadi, Preparation and Properties of Enhanced Nanocomposites Based on PLA/PC Blends Reinforced with Silica Nanoparticles, *Polym. Adv. Technol.*, 2020, **31**(3), p 566–573
37. R.B. Valapa, G. Pugazhenthil and V. Katiyar, Effect of Graphene Content on the Properties of Poly(Lactic Acid) Nanocomposites, *RSC Adv.*, 2015, **5**(36), p 28410–28423
38. M.S. Butt, A. Maqbool, M.A. Umer, M. Saleem, R.A. Malik, I.M. Alarifi and H. Alrobei, Enhanced Mechanical Properties of Surface Treated AZ31 Reinforced Polymer Composites, *Crystals*, 2020, **10**(5), p 381
39. A.Y. Patil, N.R. Banapurmath and U.S. Shivangi, Feasibility Study of Epoxy Coated Poly Lactic Acid as a Sustainable Replacement for River Sand, *J. Clean. Prod.*, 2020, **267**, p 121750
40. W. Nuthong, P. Uawongsuwan, W. Pivsa-Art and H. Hamada, Impact Property of Flexible Epoxy Treated Natural Fiber Reinforced PLA Composites, *Energy Procedia*, 2013, **34**, p 839–847
41. A.A. Yussuf, I. Massoumi and A. Hassan, Comparison of Poly(lactic Acid)/Kenaf and Poly(lactic Acid)/Rise Husk Composites: The Influence

- of the Natural Fibers on the Mechanical, Thermal and Biodegradability Properties, *J. Polym. Environ.*, 2010, **18**(3), p 422–429
42. L. Aliotta, V. Gigante, M.B. Coltelli, P. Cinelli, A. Lazzeri and M. Seggiani, Thermo-Mechanical Properties of PLA/Short Flax Fiber Biocomposites, *Appl. Sci.*, 2019, **9**(18), p 3797
 43. N.V. Kumar, N.R. Banapurmath, S.V. Ganachari, A.M. Sajjan and A.Y. Patil, Feasibility Studies on Bio Composites Using PLA and Epoxy for Structural Applications, *IOP Conf. Ser.: Mater. Sci. Eng.*, 2021, **1070**(1), p 012048
 44. A.P. Mathew and K. Oksman, Processing of bionanocomposites: solution casting, *Handbook of Green Materials*. World Scientific, Singapore, 2013, p 35–52
 45. P.M. Visakh and S. Thomas, Preparation of bionanomaterials and their polymer nanocomposites from waste and biomass, *Waste Biomass Valor.*, 2010, **1**(1), p 121–134
 46. R.K. Jena and C.Y. Yue, Development of Nanocomposite for Rigid Riser Application: Diallyl Bisphenol A Modified Bismaleimide / Epoxy Interpenetrating Network and Its Nanocomposite (NH2-MWCNT), *Compos. Sci. Technol.*, 2016, **124**, p 27–35
 47. A.Y. Patil, N.R. Banapurmath, J.S. Yaradoddi, B.B. Kotturshettar, A.S. Shettar, G.D. Basavaraj, R. Keshavamurthy, T.M. Yunus Khan and S.N. Mathad, Experimental and Simulation Studies on Waste Vegetable Peels as Bio-Composite Fillers for Light Duty Applications, *Arab. J. Sci. Eng.*, 2019, **44**(9), p 7895–7907
 48. N.P. Singh, V.K. Gupta and A.P. Singh, Graphene and Carbon Nanotube Reinforced Epoxy Nanocomposites: A Review, *Polymer*, 2019, **180**, p 121724
 49. X. Yu and H. Xu, Lightweight Composites Reinforced by Agricultural Byproducts, *Lightw. Mater. Biopolym. Biofibers*, 2014 <https://doi.org/10.1021/bk-2014-1175.ch012>
 50. G. Xu, S. Chen, X. Yan, C. Yang and Z. Chen, Synthesis and Hydrophilic Performance of Poly(Lactic Acid)-Poly(Ethylene Glycol) Block Copolymers, *Am. J. Anal. Chem.*, 2016, **07**(03), p 299
 51. L. Vanharova, M. Julinova and R. Slavik, PVP Based Materials: Biodegradation in Different Environments, *Ecol. Chem. Eng. S*, 2017, **24**(2), p 299–309
 52. M. Khakestani, S.H. Jafari, P. Zahedi, R. Bagheri and R. Hajiaghaee, Physical, Morphological, and Biological Studies on PLA/NHA Composite Nanofibrous Webs Containing Equisetum Arvense Herbal Extract for Bone Tissue Engineering, *J. Appl. Polym. Sci.*, 2017, **134**(39), p 1–10
 53. H. Lu and S.G. Kazarian, How Does High-Pressure CO₂ Affect the Morphology of PCL/PLA Blends? Visualization of Phase Separation Using in Situ ATR-FTIR Spectroscopic Imaging, *Spectrochim. Acta - Part A: Mol. Biomol. Spectros.*, 2020, **243**, p 118760
 54. C. Sun, C. Li, H. Tan and Y. Zhang, Synergistic Effects of Wood Fiber and Polylactic Acid during Co-Pyrolysis Using TG-FTIR-MS and Py-GC/MS, *Energy Convers. Manag.*, 2019, **202**(October), p 112212
 55. A.M. El-Hadi, Increase the Elongation at Break of Poly (Lactic Acid) Composites for Use in Food Packaging Films, *Sci. Rep.*, 2017, **7**(May), p 1–14
 56. L. Ramos-galicia, A. Laura, and R. Fuentes-, Enhancement of Mechanical Properties of Epoxy / Graphene Nanocomposite Enhancement of Mechanical Properties of Epoxy / Graphene Nanocomposite, n.d
 57. T. Batakliiev, I. Petrova-Doycheva, V. Angelov, V. Georgiev, E. Ivanov, R. Kotsilkova, M. Casa, C. Cirillo, R. Adami, M. Sarno and P. Ciambelli, Effects of Graphene Nanoplatelets and Multiwall Carbon Nanotubes on the Structure and Mechanical Properties of Poly(Lactic Acid) Composites: A Comparative Study, *Appl. Sci.*, 2019, **9**(3), p 469
 58. A. Kohli, S. Ishwar, M.J. Charan, C.M. Adarsha, A.Y. Patil and B.B. Kotturshettar, Design and Simulation Study of Pineapple Leaf Reinforced Fiber Glass as an Alternative Material for Prosthetic Limb, *IOP Conf. Series: Mater. Sci. Eng.*, 2020, **872**, p 012118
 59. D.N. Yashasvi, J. Badkar, J. Kalburgi, K. Koppalkar, K. Purohit, A. Patil, G. Fattepur and B.B. Kotturshettar, Simulation Study on Mechanical Properties of a Sustainable Alternative Material for Electric Cable Cover, *IOP Conf. Ser.: Mater. Sci. Eng.*, 2020, **872**, p 012016
 60. P. Kandekar, A. Acharaya, A. Chatta, A. Kamat, A.Y. Patil and B.B. Kotturshettar, A Feasibility Study of Plastic as an Alternative to Air Package in Performance Vehicle, *IOP Conf. Ser.: Mater. Sci. Eng.*, 2020, **872**, p 012076
 61. A.Y. Patil, N.R. Banapurmath, J.S. Yaradoddi, B.B. Kotturshettar, A.S. Shettar, G.D. Basavaraj, R. Keshavamurthy, T.M. Yunus Khan and S.N. Mathad, Experimental and Simulation Studies on Waste Vegetable Peels as Bio-Composite Fillers for Light Duty Applications, *Arabian J. Sci. Eng.*, 2019, **44**(9), p 7895–7907
 62. P.S. Yavagal, P.A. Kulkarni, N.M. Patil, N.S. Salimath, A.Y. Patil, R.S. Savadi and B.B. Kotturshettar, Cleaner Production of Edible Straw as Replacement for Thermoset Plastic, *Mater. Today: Proc.*, 2020, **32**, p 492–497
 63. S. Kiran Totla, A.M. Pillai, M. Chetan, C. Warad, S.K. Vinodkumar, A.Y. Patil and B.B. Kotturshettar, Analysis of Helmet with Coconut Shell as the Outer Layer, *Mater. Today: Proc.*, 2020, **32**, p 365–373
 64. H. Poornakanta, K. Kadam, D. Pawar, K. Medar, I. Makandar, A.Y. Patil and B.B. Kotturshettar, Optimization of Sluice Gate under Fatigue Life Subjected for Forced Vibration by Fluid Flow, *Strojnícky časopis—J. Mech. Eng.*, 2018, **68**(3), p 129–142
 65. E. Wang, Y. Dong, M.Z. Islam, L. Yu, F. Liu, S. Chen, X. Qi, Y. Zhu, Y. Fu, Z. Xu and N. Hu, Effect of Graphene Oxide-Carbon Nanotube Hybrid Filler on the Mechanical Property and Thermal Response Speed of Shape Memory Epoxy Composites, *Compos. Sci. Technol.*, 2019, **169**, p 209–216
 66. A. Bisht, K. Dasgupta and D. Lahiri, Evaluating the Effect of Addition of Nanodiamond on the Synergistic Effect of Graphene-Carbon Nanotube Hybrid on the Mechanical Properties of Epoxy Based Composites, *Polym. Test.*, 2020, **81**, p 106274
 67. A.A. Moosa, A. Ramazani and F. Karim Kubba, Synergetic Effects of Graphene and Nonfunctionalized Carbon Nanotubes Hybrid Reinforced Epoxy Matrix on Mechanical, Thermal and Wettability Properties of Nanocomposites, *Am. J. Mater. Sci.*, 2017, **7**(1), p 1–11
 68. A.K. Pathak, M. Borah, A. Gupta, T. Yokozeki and S.R. Dhakate, Improved Mechanical Properties of Carbon Fiber/Graphene Oxide-Epoxy Hybrid Composites, *Compos. Sci. Technol.*, 2016, **135**, p 28–38
 69. D. Bazrgari, F. Moztafzadeh, A.A. Sabbagh-Alvani, M. Rasoulian-boroujeni, M. Tahriri and L. Tayebi, Mechanical Properties and Tribological Performance of Epoxy/Al₂O₃ Nanocomposite, *Ceram. Int.*, 2018, **44**(1), p 1220–1224
 70. S.A. Hallad, N.R. Banapurmath, V. Dhage, V.S. Ajarekar, M.T. Godi and A.S. Shettar, Kevlar Reinforced Polymer Matrix Composite for Structural Application, *IOP Conf. Ser.: Mater. Sci. Eng.*, 2018, **376**(1), p 012074
 71. S.M. Suresh Kumar, D. Duraibabu and K. Subramanian, Studies on Mechanical, Thermal and Dynamic Mechanical Properties of Untreated (Raw) and Treated Coconut Sheath Fiber Reinforced Epoxy Composites, *Mater. Design*, 2014, **59**, p 63–69

Publisher's Note Springer Nature remains neutral with regard to jurisdictional claims in published maps and institutional affiliations.